



Investigating effects of phosphogypsum disposal practices on the environmental performance of phosphate fertilizer production using energy analysis and carbon emission amounting: A case study from China

Zeying Wang^a, Xiaohan Ma^a, Hengyu Pan^a, Xiangdong Yang^{b,*}, Xiaohong Zhang^{a,**}, Yanfeng Lyu^c, Wenjie Liao^d, Wei Shui^e, Jun Wu^a, Min Xu^a, Yanzong Zhang^a, Shirong Zhang^a, Yinlong Xiao^a, Hongbing Luo^f

^a College of Environmental Sciences, Sichuan Agricultural University-Chengdu Campus, Chengdu, Sichuan, 611130, PR China

^b Institute of Agricultural Resources and Regional Planning, Chinese Academy of Agricultural Sciences, Key Laboratory of Plant Nutrition and Fertilizer, Ministry of Agriculture and Rural Affairs, Beijing, 100081, PR China

^c Biogas Institute of Ministry of Agriculture and Rural Affairs, Key Laboratory of Development and Application of Rural Renewable Energy, Ministry of Agriculture and Rural Affairs, Chengdu, 610041, PR China

^d Institute of New Energy and Low-Carbon Technology, Sichuan University, Chengdu, 610065, PR China

^e College of Environment and Safety Engineering, Fuzhou University, Fuzhou, 350116, PR China

^f College of Civil Engineering, Sichuan Agricultural University- Dufiangyan Campus, Chengdu, Sichuan, 611830, PR China

ARTICLE INFO

Handling Editor: Mingzhou Jin

Keywords:

Phosphate fertilizer production

Phosphogypsum

Energy

Emissions' impact

Carbon emission

ABSTRACT

The phosphate fertilizer industry faces increasing environmental pressures related to phosphogypsum disposal. It is necessary to explore the impact of different phosphogypsum disposal schemes on the comprehensive performance to promote sustainable development in this industry. We propose a comprehensive approach based on energy analysis and carbon emission accounting to compare the impacts of different phosphogypsum disposal schemes on phosphate fertilizer production in terms of environmental sustainability, pollutant emission impacts, carbon emission intensity, and their synergistic effects. As a case study, a monoammonium phosphate production enterprise (phosphogypsum storage, Scenario 1) in Hubei Province and three other scenarios based on different phosphogypsum resource utilization practices (Scenario 2: monoammonium phosphate production + phosphogypsum manufacturing building materials; Scenario 3: monoammonium phosphate production + phosphogypsum manufacturing fertilizer filling materials; and Scenario 4: monoammonium phosphate production + phosphogypsum manufacturing cement retarder) were investigated using the proposed approach. The results show that the three phosphogypsum resource utilization practices could enhance the synergistic effect of the integrated system to different degrees relative to Scenario 1 by improving the energy-use efficiency and/or reducing the impact of pollutant emissions. Scenario 3 had the best synergistic effect, followed by scenarios 4, 2, and 1. The three phosphogypsum reuse practices enhanced carbon emission intensity to varying degrees compared with Scenario 1 due to the increasing fossil energy use. Those phosphogypsum reuse practices, based on nonrenewable resources/energy source inputs, caused conflict between waste reduction and carbon emission reduction. This study helps construct an integrated approach for thoroughly investigating the environmental performance of an integrated system consisting of phosphate fertilizer production and phosphogypsum disposal, thus providing a decision-making tool for the phosphate fertilizer industry. We also present targeted decision-making information for phosphate fertilizer production in China.

* Corresponding author.

** Corresponding author.

E-mail addresses: yangxiangdong@caas.cn (X. Yang), zxh19701102@126.com (X. Zhang).

1. Introduction

1.1. Background

Phosphorus is a strategic, limited, and nonrenewable resource. Thus, due to population growth and diet preferences, phosphorous security challenges and future shortages predictions have raised concerns (Wang et al., 2021a,b). Phosphorus fertilizer input has been the primary measure to improve the soil phosphorus supply capacity and crop yield (Du et al., 2022) with increasing intensive agricultural planting, derived from the expansion of the urban scale and the improvement in residents' consumption levels (Yang et al., 2022). China has become the largest phosphate (P) fertilizer producer in the world, accounting for approximately 40% of the total P fertilizer production in 2012 (Zhang et al., 2017), and the output will be about 13.00 million tons per year in the 14th Five-Year Plan of China (Cui et al., 2022a). However, the large-scale production of P fertilizer accelerates global fossil energy consumption and produces large amounts of phosphogypsum (PG). Statistical data showed that about 4.5 t ~5.5 t PG is produced for every 1 t of phosphoric acid (Wei et al., 2021). PG, a by-product of P fertilizer production, poses potential risks to the human health and environment during its disposal, especially when stored (Tayibi et al., 2009). The global stock of PG has exceeded 6 billion tons and will continue to grow at approximately 200 million tons per year, approximately 40% of which comes from China (Ou et al., 2021). China will have accumulated over 830 million tons of PG by 2020, occupying a large land area and posing potential environmental and safety risks (Cui et al., 2022b). However, China's comprehensive utilization rate of PG was only 38.67% in 2019, and stacking is still the primary disposal method (Ou et al., 2021). Therefore, there is an urgent need for the P fertilizer industry to implement the resource use of PG for sustainable development (Yang, 2021).

Meanwhile, proper PG waste recycling can also become a measure for promoting a sustainable P supply by reducing phosphorus loss and waste production (Ogunmoroti et al., 2022), which can act as a control for future food security (Liu et al., 2020; Yuan et al., 2018). However, the resource utilization of PG also consumes extra resources and energy sources, which can lead to secondary environmental issues. The impacts of PG resource use schemes on the performance of the P fertilizer industry should be systematically evaluated. This will help in promoting the coordinative development of the industry for green and low-carbon emission of PG resource use to align with the China's carbon neutrality goal.

1.2. Literature review

Researchers have adopted different methods to assess the performance of the P fertilizer industry. For example, Da Silva and Kulay (2005) used a life cycle assessment (LCA) to compare the environmental performance of two different phosphate fertilizer production routes in Brazil and revealed the main factors affecting their environmental performance. To explore alternative sources of phosphorus, Pradel et al. (2020) used LCA to evaluate whether sludge-based phosphate fertilizer (SBPF) can be used as an appropriate alternative to phosphate rock based on fertilizer production, and pointed out the advantages and disadvantages of SBPF. Zhang et al. (2008) used material flow analysis and economic evaluation to investigate the P fertilizer utilization efficiency and economic benefits in China's P fertilizer industry. Zhou et al. (2021) examined changes in P flow in the food chain of a typical agricultural county in China from 1980 to 2017 using substance flow analyses, and they found that increasing the recycling rate of manure P from the current 43%–95% would reduce fertilizer P use by 17% and reduced P losses by 47%. Ma et al. (2018) established a system dynamics (SD) model to evaluate the effects of different ways of applying information technology in the P fertilizer industry and found that the application of information technology can stimulate the vitality of entities in the

industry and achieve win-win results. Zhang et al. (2017) used LCA to evaluate the environmental impact of diammonium phosphate and monoammonium phosphate production in China based on national and regional statistical data. They found that the total environmental burden caused by production is mainly due to climate change, land acidification, human toxicity, particle formation, and marine ecotoxicity. These studies provide beneficial policymaking information for the environmental management of the P fertilizer industry from different perspectives. However, they ignore the environmental contribution to the industrial production and the quality differences among diverse natural resources and energy sources; thus, they do not represent a holistic picture when discussing ecological sustainability on a larger temporal and spatial scale (Björklund and GeberRydborg, 2001). Simultaneously, large amounts of PG production cause serious disposal difficulties and high management costs. This makes PG disposal one of the main issues affecting the sustainable development of P fertilizer production. Therefore, a harmless, comprehensive, and high-value utilization of PG has aroused interest in the scientific community.

Currently, the comprehensive utilization of PG is mainly carried out in agriculture, construction, and roadwork. In China, PG is mainly treated by open-air stockpiling and dumping into the sea, only a tiny portion of which is effectively utilized (Contreras et al., 2015). In the field of construction and road construction, PG can become a viable substitute for gypsum, after specific beneficiation processes (Canut et al., 2008). A new type of building material characterized by environmental high strength, waterproofing and which can also protect the environment (Wu et al., 2022), would act as a prepared product for road construction or as an additive for cement production (Valkov et al., 2014). Furthermore, it can be a raw material for self-leveling mortar (Yang et al., 2016).

Alcordo and Rechcigl (1993) reviewed the potential use of PG in agriculture-related research, including improving soil acidity (Takahashi et al., 2006) and providing F, P, S, and other elements needed for plant growth (Delgado et al., 2002; Tang et al., 2006). The research on mitigating heavy metal pollution through the adsorption and solidification of heavy metal ions in soil (Dijkstra et al., 2004), and reducing soil salinity and moisture while increasing soil fertility and topsoil organic matter has (Huang et al., 2022) also gained importance. However, these studies mainly focus on the technical feasibility of PG reuse. Few studies systematically investigated the influence of PG disposal practices on the environmental performance of P fertilizer production in terms of resource use, pollutant impacts, and carbon emissions.

Transforming by-products into resources is widely advocated to strengthen the circular economy by increasing the life cycle of resources. However, it is not always sustainable (Mohammed et al., 2018) and depends on diverse reuse methods. Reusing PG may lead to secondary environmental problems, such as fossil fuel consumption, air pollution emissions, and increased greenhouse gas emissions, which must be thoroughly evaluated. For instance, Mohammed et al. (2018) assessed the sustainability of the symbiotic process of using PG by-products in papermaking and fertilizer production. They found that PG-based paper and fertilizer are not environmentally friendly in some aspects and are not economically profitable compared to conventional products. They focused on the impacts of resource consumption and emissions but did not consider the environmental contribution to economic activities. Based on the concept of policy intervention, Cui et al. (2022b) constructed a new dynamic business model (DBM) and proposed different policy scenarios to simulate their effects on the development of PG recycling in Yichang. They also analyzed the behavior of the government, enterprises, and consumers in the PG recycling market excluding the impact of pollutants generated in PG recycling on the environment and the environmental contribution to the production. Chen et al. (2019) put forward a new comprehensive indicator, green Development Degree (GDD), based on material flow analysis, to evaluate the green degree of sulfuric acid and cement (PSC) enterprises using PG as one of the primary raw materials. However, the impact of emissions, based on

material flows, excludes the differences in diverse materials and energy sources and the environmental contribution to production. Kulczycka et al. (2016) used an LCA to evaluate and compare PG landfills and the recovery of rare earth elements (REE) from PG waste. However, emissions' impacts based on LCA do not fully consider the environmental contributions and differences in diverse materials and energy sources. Overall, the PG resource utilization process still depends on ecosystem support besides artificial contributions, but environmental services are generally ignored in the studies mentioned above, while differences in diverse resources and energy sources are also often neglected. Tsioka and Voudrias (2020) compared four alternative PG management methods using LCA, accompanied by an economic cost analysis. They reached an inconsistent conclusion: the use of PG as a soil amendment is the best option based on LCA, whereas disposal of PG in a stack is the best option based on economic cost, which could confuse policymakers. Therefore, exploring the integration of several evaluation methods is necessary to provide consistent conclusions for decision-making.

Comparatively, energy accounting can assign value to environmental efforts and artificial investments (Pan et al., 2022). This method can quantify the impact of pollutant emissions and enable distinctions between the qualities of resources so that the environmental contribution to industrial production can be properly evaluated. Energy analysis (EmA) has been widely applied to evaluate various production systems. Ali et al. (2018) used the EmA to assess the impacts of different solid waste collection and disposal programs, while Cai et al. (2018) used EmA to calculate the energy loss of industrial solid waste using different treatment methods and to measure eco-environment loss quantitatively. Wang et al. (2018) investigated the impact of waste reuse on the sustainability of a municipal solid waste incineration system using EmA. The results showed that slag reuse could significantly improve the sustainability of an integrated system. However, the EmA of the combination system (phosphate fertilizer production + PG disposal practices) and its pollutant emissions' impact have not yet been investigated.

Furthermore, there is a lack of comprehensive evaluation of the performance of the combination system in terms of resource and energy efficiencies, pollutant emission impacts, and greenhouse gas emissions. Finally, there is an urgent need for the P fertilizer industry to promote the synergistic effects of PG disposal practices based on different environmental performance indicators, considering that the Chinese government has been striving to promote co-benefits between pollution reduction and carbon emission reduction in industrial sectors. Given the background of carbon dioxide emission peaks before 2030 and carbon neutrality before 2060 (Dong et al., 2021), it is necessary to systematically investigate the influence of PG disposal practices on the environmental performance of P fertilizer production from diverse angles.

1.3. Research purpose and novelty

Food security has been highlighted in the context of the global COVID pandemic. Supply chain reform has intensified, coupled with high pressures for safety and environmental protection (Wang et al., 2021a,b). As one of the major industries responsible for national energy conservation and emission reduction, P fertilizer production should improve the efficiency of resources and energy use and minimize the final environmental emissions' impact according to the polluter's responsibility principle. This study investigated the effects of PG disposal practices on the performance of phosphorus fertilizer production using an improved EmA by considering the impacts of pollutant emissions combined with carbon emission accounting. By doing so, this study could establish a comprehensive indicator system to assess the environmental performance of an integrated system consisting of P fertilizer production and PG disposal practices from the perspective of environmental sustainability, the impact of pollution emission and carbon emission intensity, and compare the effect of different PG disposal methods on the environmental performance of the combined system for decision-making. The proposed approach was applied as a case study to

investigate four PG disposal scenarios for a monoammonium phosphate (MAP) production enterprise in Hubei Province, China, to provide targeted suggestions to decision-makers. The innovation of this study is rooted in constructing an integrated decision-making tool for the P fertilizer industry that can thoroughly investigate the environmental performance of the integrated system consisting of P fertilizer production and PG disposal practices and providing targeted decision-making information for Chinese P fertilizer production.

2. Introduction of the study case

The MAP enterprise in this study is located in Yichang City ($110^{\circ}15\text{--}112^{\circ}04\text{ E}$ and $29^{\circ} 56\text{--}31^{\circ}34\text{ N}$), southwest Hubei Province, China. The plant area of this enterprise is 7124.6 m^2 , and the total investment in this project was 95.692 million yuan. The annual output of powdered MAP is $1.80E+05\text{ t/yr}$, accompanied by $3.81E+05\text{ t/yr}$ of PG production that is given for stockpiling. Currently, China has become the largest P fertilizer producer in the world, accounting for approximately 40% of the total P fertilizer production in 2012 (Zhang et al., 2017), and MAP fertilizer accounted for approximately 37.4% of the total P fertilizer production in China (Zhang, 2016). Here, the most popular method adopted by the enterprise is the slurry method that is used for MAP production in China, and the main chemical composition of PG is similar to that of PG used worldwide. Therefore, this case is representative and has specific guiding significance for similar phosphate fertilizer manufacturers in China and other countries.

This study considers the original case as Scenario 1, which can be divided into MAP production and PG disposal stages. As shown in Fig. 1, the MAP production stage included sulfuric acid production, phosphate rock pulping, phosphoric acid production, and MAP synthesis. After crushing the phosphate rock, a phosphate rock slurry was obtained using a wet ball mill. The phosphorus ore slurry and sulfuric acid underwent an extraction reaction in the extraction tank to generate a mixed slurry of phosphoric acid and calcium sulfate crystals, which was then filtered to obtain the finished phosphoric acid and sent to the phosphoric acid storage tank. Simultaneously, the liquid ammonia was evaporated into gaseous ammonia by steam heating, ammoniated, and neutralized with diluted phosphoric acid in the neutralization reactor to obtain an ammonium phosphate slurry. After the ammonium phosphate slurry overflowed into the evaporation feed tank, it entered the II-effect evaporation system for an initial concentration and then entered the I-effect evaporation system to concentrate again to satisfy the specified concentration. Finally, MAP powder was obtained after spray drying, cooling, and packaging. The PG produced from the phosphoric acid was sent to the slag yard for storage. Due to the surplus production capacity of sulfuric acid installation in the project, some sulfuric acid was sold. The wastewater produced in the MAP production stage and the leachate produced in the PG slag yard were pretreated to satisfy the 'Discharge standard of water pollutants for the phosphate fertilizer industry' (GB 15580–2011). They entered the sewage treatment station for further treatment. Air pollutants produced during production included dust, fluoride, ammonia, sulfuric acid mist, and SO_2 . Among these, sulfuric acid mist and SO_2 were discharged after satisfying the emission standards of pollutants for the sulfuric acid industry (GB 26132–2010), ammonia is emitted into the atmospheric environment after satisfying the emission standards for odor pollutants (GB 14554–93) and the remaining air pollutants are emitted after satisfying the Integrated Emission Standard of Air Pollutants (GB16297-2004). Other by-products, including sulfur slag and coal slag, are sold to other enterprises for comprehensive utilization, which is beyond the scope of this study.

According to the current utilization of PG in China, three standard PG resource utilization methods, i.e., producing gypsum powder and gypsum block using PG, producing fertilizer filling material using PG, and producing cement retarder using PG, were selected to construct other three scenarios to investigate impacts of these resources utilization

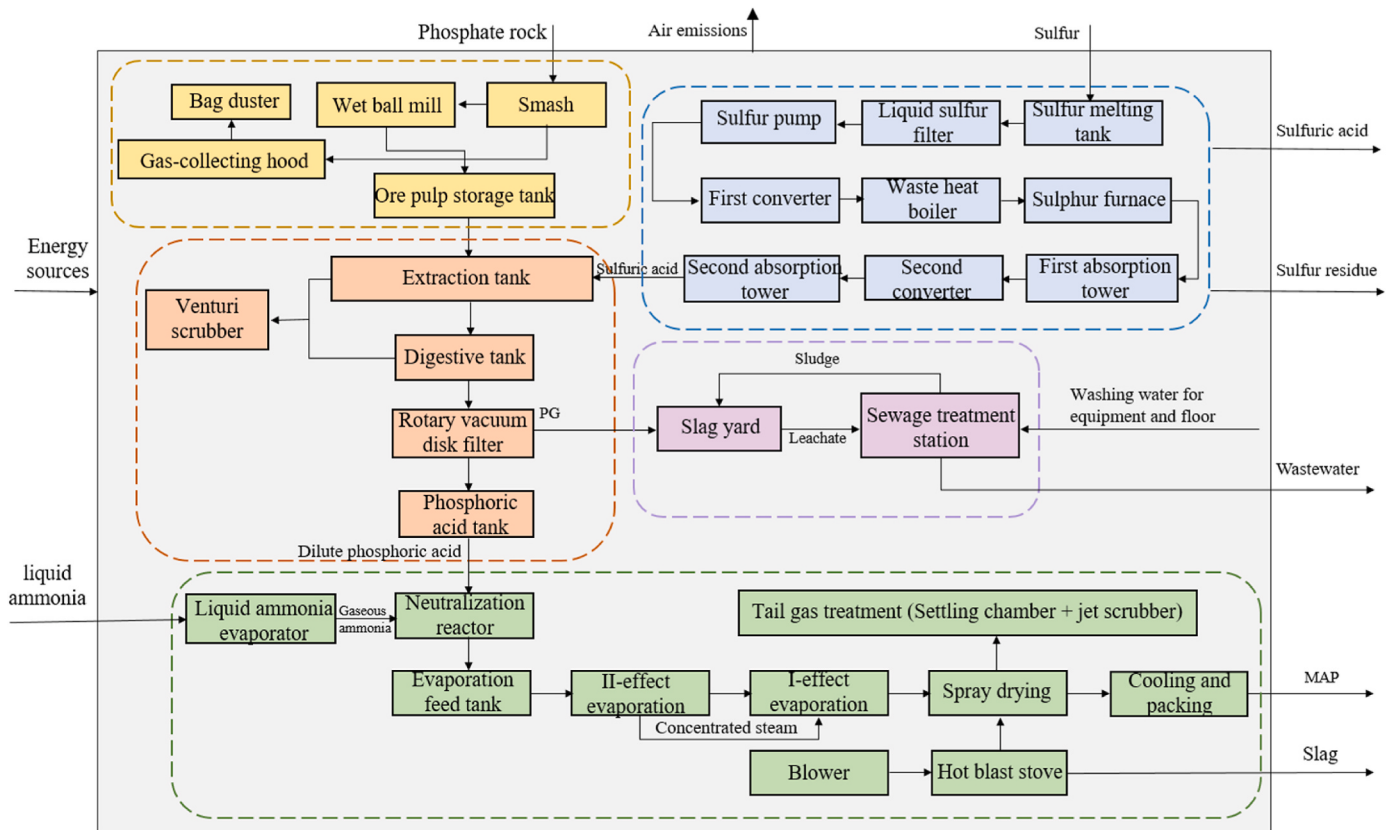


Fig. 1. The technological process of Scenario 1.

ways on the performance of the MAP production system relative to Scenario 1, named as Scenario 2, Scenario 3 and Scenario 4, respectively. Only the PG disposal ways change, but the MAP production stage remains the same in the four scenarios. Scenario 2: PG was used to

produce gypsum powder and blocks. Gypsum powder has good gel strength and can be used for preparing gypsum-based building materials (Gao et al., 2022). As a new wall material, a gypsum block has the advantages of fire prevention, environmental protection, renewability, and

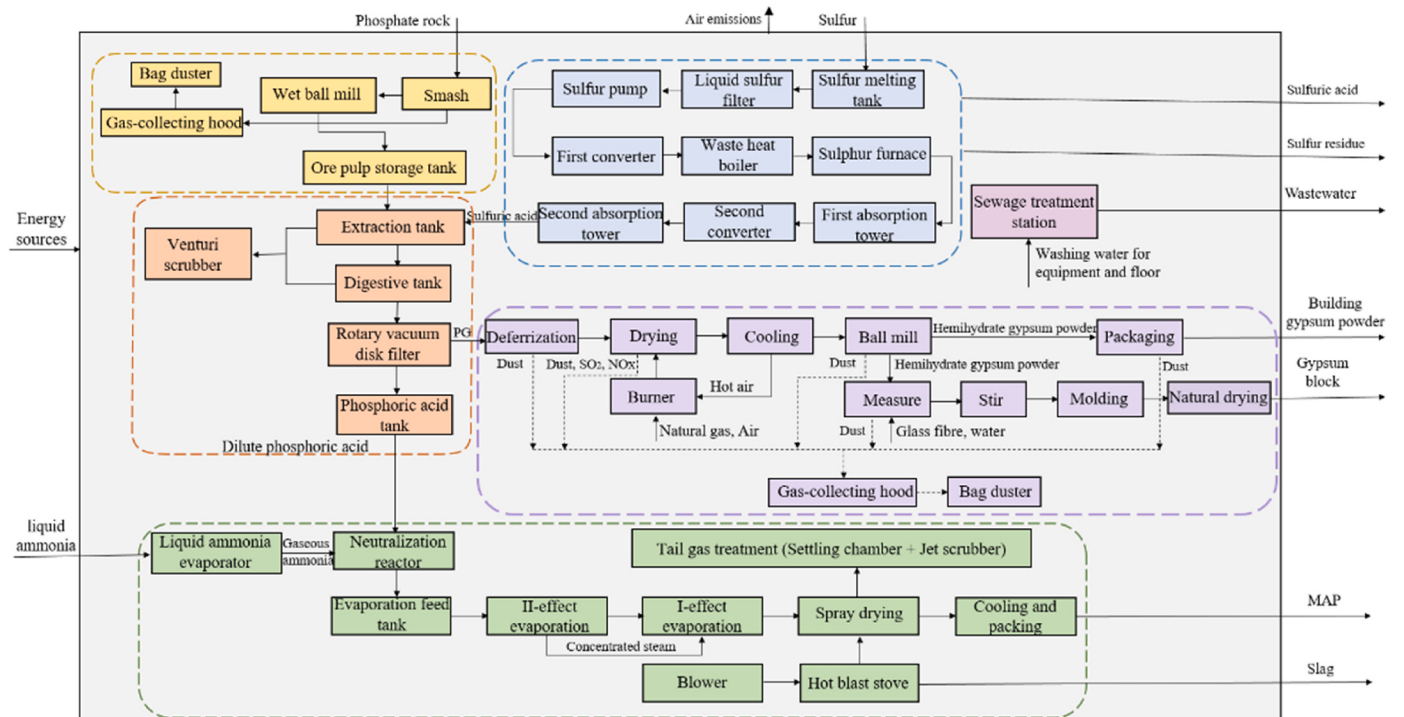


Fig. 2. The technological process of Scenario 2.

good workability (Jia et al., 2019). The preparation of gypsum blocks with PG as raw material makes full use of PG, meets the needs of large-scale construction production, and has formed a specific production capacity (Lou et al., 2019). The entire process of Scenario 2 is shown in Fig. 2. The PG from the MAP production stage was pretreated and then sent to a rotary kiln for drying after iron removal using a permanent magnetic separator. Free and crystal water was removed by drying with dihydrate PG to generate hemihydrate PG. After cooling, the hemihydrate PG was sent to the modified ball mill to increase the specific surface area of the PG powder and the flexural and compressive strengths of the product. Finally, the finished product, building gypsum powder, was obtained. Part of the building gypsum powder was packed for sale, and the rest was used as a raw material for producing gypsum blocks. First, the raw materials (hemihydrate gypsum powder and glass fibers) were measured using an electronic scale and sent to a high-speed mixer to evenly mix the components. Subsequently, the slurry was poured into each chamber of the molding machine automatically, and finally, the gypsum blocks were formed after natural drying. The production wastewater is mainly from ground and equipment cleaning and monitoring analysis. It is first precipitated by a neutralization sedimentation tank and then completely reused for gypsum block production. After treatment by a bag filter, all air emissions, including dust, SO₂, and others, were emitted according to the integrated emission standard of air pollutants (GB16297-2004).

Scenario 3: PG was used as a raw material to produce the fertilizer-filling material. PG contains phosphorus, magnesium, calcium, iron, zinc, manganese, and other essential elements required for crop growth; therefore, act as a raw material for producing medium- and trace-element fertilizers (Xu and Zhang, 2017). The process flow for Scenario 3 is shown in Fig. 3. The PG from MAP production was first crushed to obtain PG powder. PG powder, fertilizer-grade dicalcium phosphate, phosphate tailings, organic matter, and lime were prepared in corresponding proportions. Next, the loader placed these raw materials into the mixer, and the granular fertilizer filling material was obtained after being mixed evenly. Finally, the mixed material is milled using a Raymond mill to obtain the final product, fertilizer-filling material. The air pollutants produced were mainly dust; thus, satisfying the

integrated emission standard of air pollutants (GB 16297–2004), with no wastewater produced. Domestic sewage is collected using dry toilets, regularly cleaned, and used for local agricultural irrigation.

Scenario 4: PG produces cement retarders in place of natural gypsum. About 30% of China's PG is one of the primary raw materials for cement retarder production (Cui et al., 2022b). As shown in Fig. 4, after the PG from MAP production was sent to the primary aggregate bin through the belt conveyor, the lumps were crushed in the disperser, and the crushed material entered the secondary aggregate bin for raw material ratio adjustment. Next, the prepared PG and lime were mixed in an intermittent double-shaft mixer for approximately 60 s. After mixing all materials, the cement retarder was obtained through natural curing in the product area. The dust generated in the production process was treated using a bag filter, and the recovered dust was returned to the production process as supplementary material. The air pollutant emissions met the secondary standard of the Integrated Emission Standard of Air Pollutants (GB16297-2004). No wastewater was discharged during the production of the cement retarder.

3. Methods

3.1. System boundary

As shown in Fig. 5, the analysis boundary starts with the raw materials and energy sources entering the production process and ends with products leaving the factory gates. Its main inputs include raw materials, energy sources, labor, and service, and its outputs include products and environmental emissions (such as fluorides (including SiF, HF, and HSiF), sulfur dioxide, ammonia, and solid waste). In contrast, inputs related to infrastructure are excluded because of the unavailability of the data. However, compared with the overall environmental burden, the environmental effect generated by infrastructure is low (Ecoinvent Center, 2010). Therefore, this exclusion did not significantly affect the results.

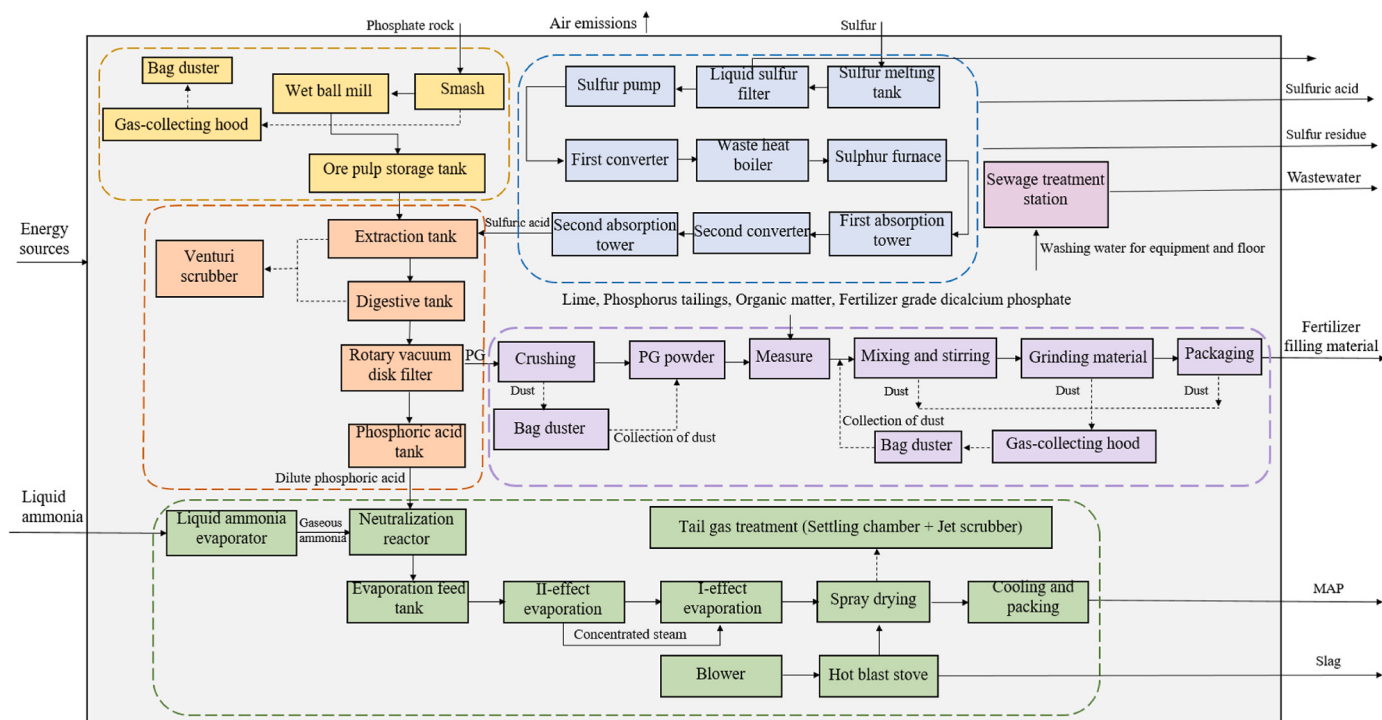


Fig. 3. The technological process of Scenario 3.

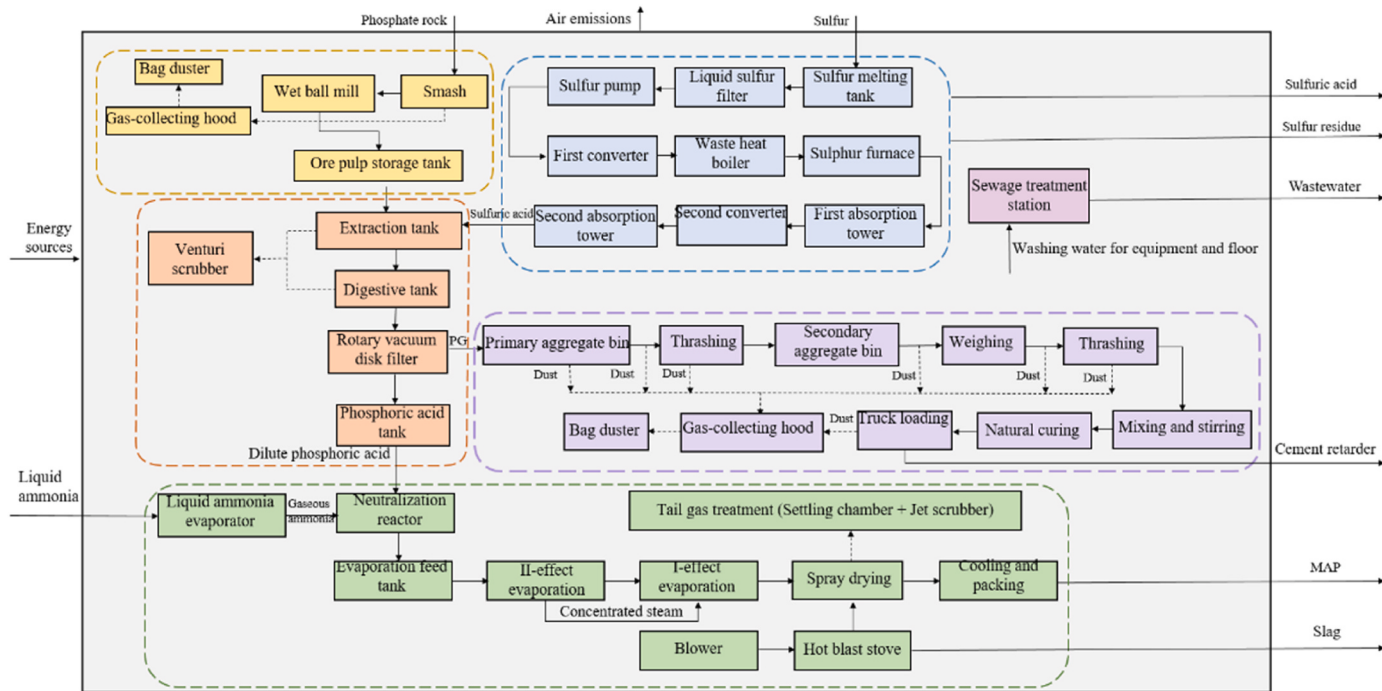


Fig. 4. The technological process of Scenario 4.

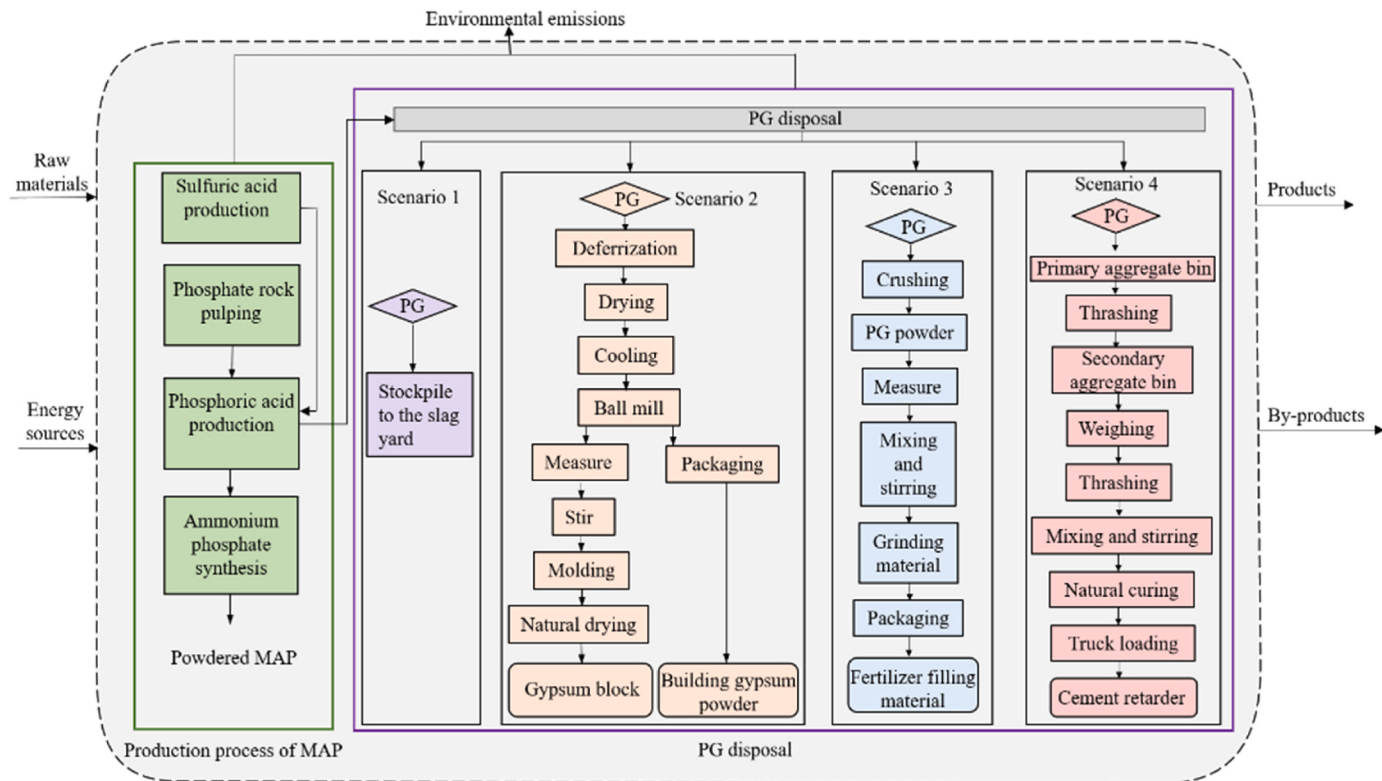


Fig. 5. The analysis boundary of this study.

3.2. EmA

Energy is the sum of all available energy inputs directly or indirectly required for a process that provides a given product or flow in terms of the same form of energy (Odum, 1988). Thus, EmA quantifies the total energy and material flow required to support a system in solar energy

joules (sej) (Odum, 1996). Unit energy value (UEV), one primary coefficient in EmA, is defined as the equivalent solar energy required to generate a unit output, usually using sej/J (energy per unit of energy), sej/g (energy per unit of mass) or sej/CNY (energy per unit of currency). The energy value of each input type can be calculated by multiplying its quantity by the corresponding UEV. In this study, the

final local renewable energy value is chosen as the sum of the primary energy sources and the largest one among the second and third energy sources (Brown and Ulgiati, 2016). The purchased inputs are further divided into purchased renewable resources (F_R) and purchased nonrenewable resources (F_N) (Wang et al., 2017). Because different energy baselines have appeared in recent years (Brown and Ulgiati, 2010; Brown et al., 2016; Campbell, 1998; Odum, 1996, 2000), the latest energy baseline, that is, $12.0E+24$ sej/yr (Brown et al., 2016) is adopted to maintain the consistency of energy accounting. After accounting for energy, system performance can be further evaluated using specific energy-based indicators (Lu and Chen, 2014).

3.2.1. Energy flows of an integrated MAP production system

As shown in Figs. 6–9, for an integrated MAP production system, composed of MAP production and PG disposal, the total energy inputs include local renewable inputs (R_1) from the local environment and purchased inputs from the economic system. According to Ref. (Shao and Chen, 2016), the renewable and nonrenewable parts of investment and operating expense are distinguished, and their ratio is approximately 0.02/0.98, respectively (The National Environmental Accounting Database (NEAD)). The outputs included products (Y, MAP- and PG-related products) and environmental emissions. These emissions may cause the following impacts: emissions require ecological services to render them harmless, and the required energy is denoted as R_2 , emissions may lead to some ecological losses, such as fish kill, water body eutrophication before reaching acceptable levels, and energy loss is denoted as R_3 , which is not considered in this study because of the lack of corresponding primary data. At the same time, pollutant emissions may also cause economic losses (L), such as harm to human health (L_H) and land occupation (L_L). The energy flow system diagrams of scenarios 1–4 are depicted in Figs. 6–9, respectively.

3.2.2. Calculating pollutant emissions' impacts

3.2.2.1. Quantifying additional ecological services. Ulgiati and Brown (2002) first proposed a method for computing local extra ecological services for diluting air pollutants, and Zhang et al. (2009) popularized this method for calculating additional local ecological services required for diluting air and water pollutants. First, the required mass of diluted air/water can be computed using Eq. (1).

$$M_{i, \text{air/water}} = d \times \frac{W_i}{c_i} \quad (1)$$

Where $M_{i, \text{air/water}}$ is the mass of air/water required to dilute the i-th pollutant, and d is the density of air/water. The air density is 1.29 kg/m³,

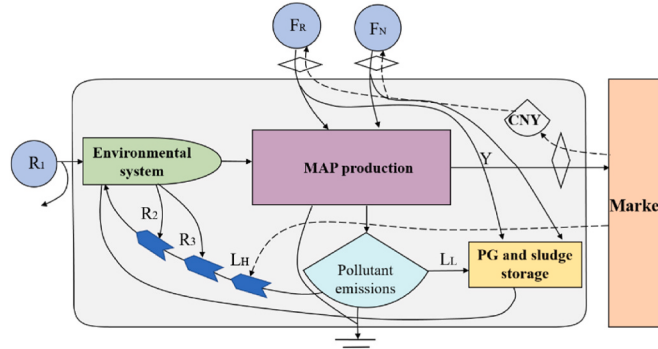


Fig. 6. Energy flow diagram of Scenario 1. R_1 : the local renewable resource inputs; F_R : the purchased renewable resource inputs; F_N : the purchased nonrenewable resource inputs; Y : energy of product; R_2 : energy of ecological services needed to dissipate pollutant emissions; R_3 : energy of the ecological loss caused by the emissions; L_H : the human health loss. L_L : energy loss caused by land occupation due to solid waste disposal. Unit: sej/yr.

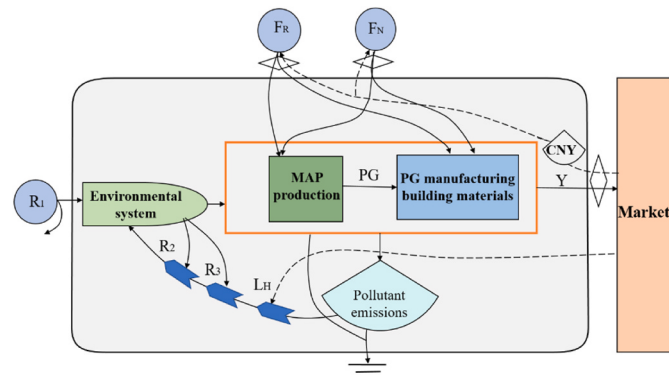


Fig. 7. Energy flow diagram of Scenario 2. R_1 : the local renewable resource inputs; F_R : the purchased renewable resource inputs; F_N : the purchased nonrenewable resource inputs; Y : energy of product; R_2 : energy of ecological services needed to dissipate the emissions; R_3 : energy of the ecological loss caused by the emissions; L_H : the human health loss. Unit: sej/yr.

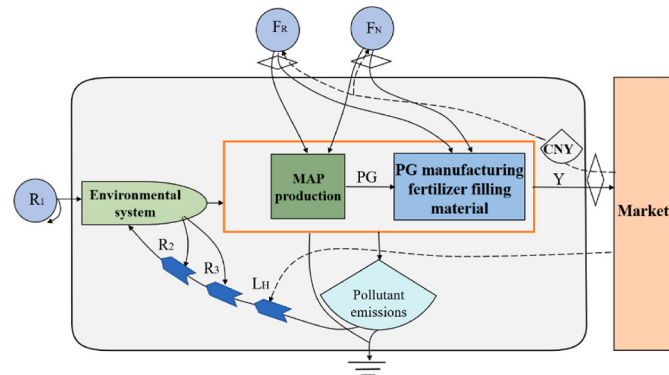


Fig. 8. Energy flow diagram of Scenario 3. R_1 : the local renewable resource inputs; F_R : the purchased renewable resource inputs; F_N : the purchased nonrenewable resource inputs; Y : energy of product; R_2 : energy of ecological services needed to dissipate the emissions; R_3 : energy of the ecological loss caused by the emissions; L_H : the human health loss. Unit: sej/yr.

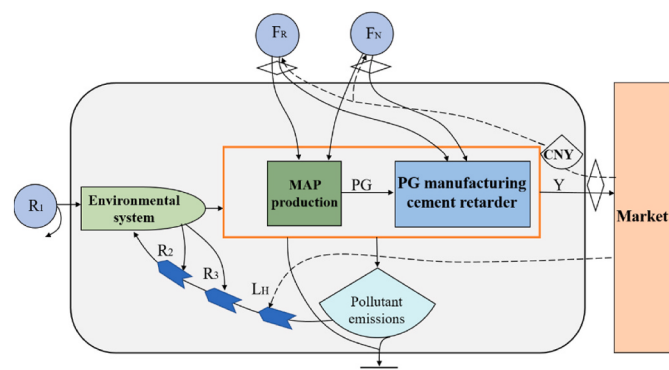


Fig. 9. Energy flow diagram of Scenario 4. R_1 : the local renewable resource inputs; F_R : the purchased renewable resource inputs; F_N : the purchased nonrenewable resource inputs; Y : energy of product; R_2 : energy of ecological services needed to dissipate the emissions; R_3 : energy of the ecological loss caused by the emissions; L_H : the human healthy loss. Unit: sej/yr.

m^3 , and the water density is 1.00 kg/L; W_i is the annual emission of the i-th air/water pollutant (kg); c_i represents the acceptable concentration of the i-th air/water pollutant, which can be cited from related environmental quality standards.

Then, the energy of extra ecological services can be determined by the kinetic energy of the dilution air or the chemical energy of the dilution water multiplied by the corresponding UEV, according to Eqs. (2) and (3) (Pan et al., 2022).

$$R_{i,air} = \frac{1}{2} \times M_{i,air} \times v^2 \times UEV_{air} \quad (2)$$

$$R_{i,water} = M_{i,water} \times \rho \times UEV_{water} \quad (3)$$

where $R_{i,air}$ and $R_{i,water}$ represent the ecological services needed for diluting the i -th air emission (sej/yr) and i -th water pollutant (sej/yr), respectively, v is the annual mean wind speed, UEV_{air} represents the transformity of wind energy ($1.91E+03$ sej/J, corrected to the baseline $12.0E+24$ seJ/yr) (Ulgiati and Brown, 2002), ρ is Gibbs free energy of water ($4.94E+03$ J/kg), and UEV_{water} is the transformity of river water ($3.54E+04$ sej/J, corrected to the baseline $12.0E+24$ seJ/yr) (Chen et al., 2022).

As air and water can dilute different pollutant emissions in the same medium, the total ecological service equals the sum of the most significant values of $R_{i,air}$ and $R_{i,water}$, as shown in equation (4).

$$R_2 = \max(R_{i,air}) + \max(R_{i,water}) \quad (4)$$

3.2.2.2. Quantifying energy loss resulting from pollutant emissions. In contrast to ecological services, energy loss can be regarded as additional economic resource compensation required to eliminate these negative impacts (Liu et al., 2017). This study did not consider ecological loss (R_3) because of the unavailability of related primary data. The energy loss to human health caused by the pollutant discharge was calculated using equation (5).

$$L_H = \sum_{i=1}^n M_i \times DALY_i \times \tau_H \quad (5)$$

where L_H represents the healthy human loss (sej/yr), M_i refers to the mass of the i -th pollutant emission (kg/yr), $DALY_i$ stands for Disability Adjusted Life Year derived from pollutant emissions' impacts on human health (person·yr/kg) (cited from the eco-indicator 99), τ_H represents the annual energy use per capita in a country or region, and τ_H is the annual gross energy value/total population of a country or region. The specific method for calculating this is as follows:

$$\tau_H = REM_{2020} \times GDP_{2020} \div Pop_{2020} \quad (6)$$

$$REM_{2020} = REM_{2015} \times \left[\frac{IGDP_{2020}}{IGDP_{2015}} \div \frac{GDP_{2020}}{GDP_{2015}} \right] \quad (7)$$

$$REM_{2015} = TEU_{2015} \div GDP_{2015} \quad (8)$$

Where REM_{2020} and REM_{2015} stand for the ratios of energy to money in 2020 and 2015 (sej/CNY), respectively. TEU_{2015} refers to the total energy used in 2015, derived from National Environmental Accounting Database. NEAD Data by Country China (2015) and GDP_{2015} stands for the gross domestic product in 2015, coming from National Bureau of statistics of China (2015). After calculating $REM_{2015} = 4.30E+11$ sej/CNY. $IGDP_{2020}$ and $IGDP_{2015}$ stand for the indexes of gross domestic product in 2020 and 2015 based on 1978, derived from National Bureau of statistics of China (2020), respectively, GDP_{2020} is the gross domestic product in 2020, and Pop_{2020} is the total population in 2020, derived from National Bureau of statistics of China (2020). After calculating, $REM_{2020} = 2.79E+11$ sej/CNY, $\tau_H = 2.00E+16$ sej/(person·yr).

Land occupation can be used to describe the impact of solid waste landfilling on the economy, and the related energy loss can be computed using Eq. (9).

$$L_L = \frac{M_S}{2.85E+04} \times \tau_L \quad (9)$$

where L_L represents the energy loss derived from land occupation (sej/yr); M_S refers to the amount of solid waste disposed of using landfill (t/yr); $2.85E+04$ means that $2.85E+04$ t industrial solid wastes approximately occupy a land area of 1 ha (t/ha; Wang et al., 2006); τ_L represents the unit energy value of the land area, which is $1.01E15$ sej/ha (Odum, 2000).

Finally, the total economic loss (L) energy was obtained using Eq. (10).

$$L = L_H + L_L \quad (10)$$

3.2.3. The corresponding energy-based indicators

According to the characteristics of the system and the research purposes of this study, the following indicators were established to describe the performance of the system.

(1) Energy yield ratio (EYR)

EYR is equal to the sum of the local renewable, local nonrenewable, and purchased energy inputs divided by the purchased energy (Eq. (11)). It is used to assess the economic benefits or competitive ability of a system (Odum, 1996). A higher indicator value reflects a better economic benefit or stronger completion ability.

$$EYR = \frac{R + N + F_R + F_N}{F_N + F_R} \quad (11)$$

(2) The environmental load ratio (ELR)

The ELR is the total nonrenewable energy input divided by the total renewable energy input (Eq. (12)). It is used to evaluate environmental pressure of a system (Odum, 1996). A higher indicator value indicates significant pressure on the local environment.

$$ELR = \frac{N + F_N}{R + F_R} \quad (12)$$

(3) Energy sustainability index (ESI)

The ESI is defined as the ratio of the EYR to the ELR (Ulgiati and Brown, 1998), as shown in Eq. (13). The ESI describes the economic output per unit of environmental load. A higher index value indicates a higher level of sustainability. According to Ref. (Ukidwe and Bakshi, 2004), when $ESI < 1$, processes and products are unsustainable in the long term; when $1 < ESI < 5$, the system may make sustainable contributions to the economy in the medium term, and in the long term, it can be considered sustainable when $5 < ESI < 10$.

$$ESI = \frac{EYR}{ELR} \quad (13)$$

(4) Pollutant emissions' impact intensity (PEI)

A PEI indicator is proposed for comparing the impacts of different scenarios on pollutant emissions. It is defined as the total energy of pollutant emissions' impacts per year divided by the annual product output, as shown in Eq. (14).

$$PEI = \frac{L + R_2 + R_3}{M_n} \quad (14)$$

where M_n is the annual product output (kg/yr). A higher indicator value indicates a higher pollutant emissions' impact per unit product of one system in the study. This indicator relates to the structure of resources and energy sources, their efficiency, and pollutant control levels.

3.3. Carbon emission accounting

Currently, there are three internationally recognized carbon emission (CE) accounting methods: the material balance algorithm, the measurement method, and the carbon emission factor method (Xiao, 2021). This study adopts the accounting method described in the national standard “greenhouse gas emissions accounting and reporting requirements-Part 10: Chemical production enterprises” (GB/T32151.10–2015).

The accounting boundary is the greenhouse gases emitted from the production of phosphate fertilizer to the following disposal of PG. The sources of carbon emissions are considered to include fossil fuel combustion, production processes, purchased net electric power, and purchased heat. Here, CE represents the sum of greenhouse gases emitted in terms of the CO₂ equivalent (CO₂-eq), which can be calculated using Eq. (15).

$$CE = CE_f + CE_p + CE_e + CE_h \quad (15)$$

where CE_f is the CO₂ emissions from fossil fuel use (t CO₂-eq); CE_p is the CO₂ emissions from the production process (t CO₂-eq), CE_e is the CO₂ emissions from the generation of purchased electricity (t CO₂-eq), and CE_h is the CO₂ emissions from the generation of purchased heat (t CO₂-eq). CE_f was calculated according to Eq. (16).

$$CE_f = \sum_{i=1}^n NCV_i \times FC_i \times CC_i \times OF_i \times \frac{44}{12} \quad (16)$$

Where NCV_i represents the average low calorific value per unit of the i-th fossil fuel (GJ/t for solid and liquid fuels, or GJ/(10E+4 Nm³) for gaseous fuels); FC_i represents the net consumption of the i-th fossil fuel (t for solid and liquid fuels, 10E+4 Nm³ for gaseous fuels); CC_i represents the carbon content per unit of calorific value of the i-th fossil fuel (t C/GJ); OF_i represents the carbon oxidation rate of the i-th fossil fuel (%); $\frac{44}{12}$ represents the ratio of relative molecular mass of CO₂ to carbon. The fossil fuels used in the system include coal, natural gas, and diesel. Here, CE_p is mainly composed of CO₂ emissions released from the chemical reaction between the carbonate carried by the raw material phosphate rock and sulfuric acid, and it is calculated using Eq. (17).

$$CE_p = MP \times 5\% \quad (17)$$

where MP represents the mass of phosphate rock; 5% is the CO₂ content of phosphate rock itself (Zhang et al., 2011). CE_e is calculated using Eq. (18).

$$CE_e = AD_e \times EF_e \quad (18)$$

where AD_e represents the net electricity consumption by enterprises (MWh), which is the difference between the amount of electricity purchased by enterprises and that generated by thermal recovery, and EF_e is the CO₂ emission factor of the electricity supply (kg CO₂-eq/kWh). Here, the latest weighted average CO₂ emission factor of the electricity supply in Central China was adopted (Xiao, 2021), which is 0.5721 kg CO₂/(kWh).

Regarding CE_h, considering that the purchased heat in the entire system is only steam, only the net purchased steam is considered. CE_h can be calculated using Eq. (19).

$$CE_h = Ma_{st} \times En_{st} \times EF_h \quad (19)$$

where Ma_{st} represents the mass of the net steam consumption (kg), En_{st} represents the energy conversion factor of steam (2.58 MJ/kg; Chen et al., 2022); EF_h stands for the CO₂ emission factor of heat production (0.11 kgCO₂/MJ; Xiao, 2021).

Furthermore, the carbon emission intensity indicator (CEI, kg CO₂-e/t product) is adopted to describe carbon emissions per unit product. It is defined as the total carbon emissions divided by product output (PO),

calculated using Eq. (20). A higher indicator value indicates a higher carbon emission intensity, and increasingly strict carbon emission control policies could limit the related product.

$$CEP = CE/PO \quad (20)$$

3.4. Synergistic effect index

An industrial system should have a higher ESI, lower PEI, and smaller CEI based on this industry's average level to promote sustainable industrial production development. This can be described using the synergistic effect index (SEI). Therefore, this index is positively related to ESI but negatively related to PEI and CEI. Each indicator value in each scheme was divided by the average value of the related indicators of all schemes to normalize the indicator values measured in different units. The SEI was then calculated using Eq. (21).

$$SEI_i = \frac{ESI_i/ESI_{av}}{(PEI_i/PEI_{av}) \times (CEI_i/CEI_{av})} \quad (21)$$

where ESI_i, PEI_i, and CEI_i refer to the indicator values of the energy sustainability index, pollutant emissions' impact intensity, and carbon emission intensity of the i-th scenario, respectively; ESI_{av}, PEI_{av}, and CEI_{av} refer to the average indicator values of the energy sustainability index, pollution emissions' impact intensity, and carbon emission intensity of all scenarios, respectively. This index is affected by resource structure and efficiency, energy mix and efficiency, pollutant control level, and degree of carbon capture and use. The larger the index value of the SEI, the higher the co-benefit of the i-th scenario among its resource efficiency, pollutant control, and carbon emission reduction. To further investigate the degree of influence of one indicator on SEI, an indicator ID was proposed according to Ref. (Cao et al., 2022) and was calculated using Eq. (22)

$$ID_i = \frac{SEI_{i,a} - SEI_{i,b}}{SEI_{i,b}} \quad (22)$$

ID_i refers to the degree of influence of the i-th indicator on the SEI, and SEI_{i,b} and SEI_{i,a} represents the indicator values of the SEI before and after considering the i-th indicator. A higher indicator value indicates a larger contribution of one indicator to the SEI when the value of ID > 0. The larger the absolute value of ID, the greater the adverse influence of an indicator on the SEI when the value of ID < 0; when the value of ID = 0, it indicates no effect of an indicator on the SEI.

3.5. Data sources and statistical tools

The required primary data were obtained from a feasibility study report, technical consultations, and related literature. The economic data were converted to 2020 using the price index for comparative analysis. The related UEVs were obtained from energy-related references and the database (SM-1), and those lacking UEVs were calculated as given in Supplementary Materials (SM-2 and 3). Combined with the introduction of the case in Section 2, data quality satisfies data robustness and evidence (Salemdeeb et al., 2021), including reliability, completeness, technological, geographical, and time-related representativeness.

This study used Microsoft Excel 2019 for data processing and charting, and technical flow charts and energy flow systematic diagrams were drawn using Microsoft PowerPoint 2019.

4. Results

4.1. Energy evaluation of the four scenarios

4.1.1. Energy flows

The energy evaluation tables for Scenarios 1–4 are provided in SM-4–7, and their energy flows are summarized in Tables 1–3. The total

Table 1

Summary of total energy flows of four scenarios, their shares and change rates of shares.

Item	R ₁ (sej/yr)	F _R (sej/yr)	F _N (sej/yr)	Total input (sej/yr)
Scenario 1	3.08E+19	3.24E+18	1.07E+21	1.10E+21
Share	2.79%	0.29%	96.92%	100.00%
Scenario 2	3.73E+19	3.76E+18	1.10E+21	1.14E+21
Share	3.28%	0.33%	96.39%	100.00%
Change rates	17.63%	12.48%	-0.54%	3.15%
Scenario 3	3.08E+19	3.01E+20	3.06E+21	3.39E+21
Share	0.91%	8.89%	90.20%	100.00%
Change rates	-67.46%	2927.42%	-6.93%	207.33%
Scenario 4	3.08E+19	3.45E+18	1.15E+21	1.18E+21
Share	2.60%	0.29%	97.10%	100.00%
Change rates	-6.58%	-0.40%	0.19%	7.05%

Note: Change rates = (The share of Scenario i – The share of Scenario 1) × 100% / the share of Scenario 1. Here i = 2, 3, 4.

energy input of Scenario 1 was 1.10E+21 sej/yr, in which the MAP production stage and the PG storage stages contributed 99.94% and 0.06%, respectively. During the MAP production stage, R₁, F_R, and F_N accounted for 2.79%, 0.29%, and 96.92% of the total energy input, respectively. Therefore, R₁ mainly came from the air, F_R was mainly derived from the renewable part of the operation cost, followed by hydropower, and F_N was mainly from phosphate rock, liquid ammonia, and the nonrenewable part of the operation cost. F_R and F_N accounted for 1.75% and 98.25% of the total energy input during the PG storage stage, respectively. Therefore, F_R mainly originated from the renewable part of the investment cost, followed by the renewable part of the operation cost. F_N mainly originated from the nonrenewable part of the investment cost, followed by lime. As far as the energy input of the whole system was concerned, phosphate rock accounted for the largest share of total energy input (52.30%), followed by liquid ammonia (20.68%), the nonrenewable part of operating costs (9.71%), sulfur (4.89%), phosphoric acid (4.58%), air (2.79%), coal (2.09%), and vanadium catalyst (2.06%); the other resources and energy sources contributed to less than 1%.

As for Scenario 2, the total energy input was 1.14E+21 sej/yr, of which the MAP production stage and the PG manufacturing building materials stages contributed 96.89% and 3.11%, respectively. During the MAP production stage, R₁, F_R, and F_N accounted for 2.79%, 0.29%, and 96.92% of the total energy input, respectively. Therefore, R₁ mainly came from the air, F_R mainly came from the renewable part of the operation cost, followed by hydropower, and F_N mainly came from

phosphate rock, liquid ammonia, and the nonrenewable part of the operational cost. In the PG manufacturing building material stage, R₁, F_R, and F_N accounted for 18.52%, 1.50%, and 79.98% of the total energy input, respectively. Therefore, R₁ mainly came from the air; F_R was mainly derived from hydropower, followed by the renewable part of the operation cost; and F_N was mainly from natural gas, followed by the nonrenewable part of the operation cost, then thermal power. As far as the energy input of the whole system is concerned, phosphate rock accounts for the largest share (50.71%), followed by liquid ammonia (20.05%), the nonrenewable part of operating costs (10%), sulfur (4.74%), phosphoric acid (4.44%), air (2.70%), coal (2.02%), vanadium catalyst (2.00%), and natural gas (1.55%); share of other resources and energy sources is less than 1%.

As for Scenario 3, the total energy input was 3.39E+21 sej/yr, of which the MAP production stage and the PG manufacturing fertilizer filling materials stages contributed 32.52% and 67.48%, respectively. During the MAP production stage, R₁, F_R, and F_N accounted for 2.79%, 0.29%, and 96.92% of the total energy input, respectively. Therefore, R₁ mainly came from the air; F_R was mainly derived from the renewable part of the operation cost, followed by hydropower, while F_N was mainly derived from phosphate rock, liquid ammonia, and the nonrenewable part of the operation cost. F_R and F_N contributed 13.03% and 86.97%, respectively, of the total energy input at the PG manufacturing fertilizer filling materials stage. Therefore, F_R mainly came from phosphorus tailings, followed by the renewable part of the operation cost, whereas F_N was mainly derived from fertilizer-grade dicalcium phosphate, followed by organic matter and the nonrenewable part of the operational cost. As far as the energy input of the whole system is concerned, fertilizer-grade dicalcium phosphate accounts for the largest share of the total energy input (54.44%), followed by phosphate rock (17.02%), phosphate tailings (8.76%), liquid ammonia (6.73%), the nonrenewable part of the operating cost (4.63%), organic matter (2.12%), sulfur (1.59%), and phosphoric acid (1.49%); other resources and energy sources contribute to less than 1%.

As for Scenario 4, the total energy input was 1.18E+21 sej/yr, of which the MAP production stage and the PG manufacturing cement retarder stages contributed 93.36% and 6.64%, respectively. During the MAP production stage, R₁, F_R, and F_N accounted for 2.79%, 0.29%, and 96.92% of the total energy input, respectively. Therefore, R₁ mainly came from the air; F_R was mainly from the renewable part of the operation cost, followed by hydropower; and F_N was mainly derived from phosphate rock, liquid ammonia, and the nonrenewable part of the operation cost. In the PG manufacturing cement retarder stage, F_R and

Table 2

Change rates of different kinds of energy flows in the four scenarios.

Item	Scenario 1	Scenario 2	Change rate	Scenario 3	Change rate	Scenario 4	Change rate
R ₁ (sej/yr)	3.08E+19	3.73E+19	21.33%	3.08E+19	0.00%	3.08E+19	0.00%
F _R (sej/yr)	3.24E+18	3.76E+18	16.02%	3.01E+20	9204.21%	3.45E+18	6.62%
F _N (sej/yr)	1.07E+21	1.10E+21	2.59%	3.06E+21	186.03%	1.15E+21	7.25%
Total input (sej/yr)	1.10E+21	1.14E+21	3.15%	3.39E+21	207.33%	1.18E+21	7.05%

Note: Changes rate = (The energy value of Scenario i – The energy value of Scenario 1) × 100% / The energy value of Scenario 1. Here i = 2, 3, 4.

Table 3

Statistics of energy flows in MAP production stage and PG disposal stage of the four scenarios.

Item	R ₁		F _R		F _N		Total input (sej/yr)
	Energy (sej/yr)	Share (%)	Energy (sej/yr)	Share (%)	Energy (sej/yr)	Share (%)	
MAP production stage (keeping the same for the four scenarios)							
Scenarios 1–4	3.08E+19	2.79%	3.23E+18	0.29%	1.07E+21	96.92%	1.10E+21
PG disposal stage							
Scenario 1	0.00E+00	0.00%	1.22E+16	1.75%	6.85E+17	98.25%	6.98E+17
Scenario 2	6.56E+18	18.52%	5.31E+17	1.50%	2.83E+19	79.98%	3.54E+19
Scenario 3	0.00E+00	0.00%	2.98E+20	13.03%	1.99E+21	86.97%	2.29E+21
Scenario 4	0.00E+00	0.00%	2.27E+17	0.29%	7.82E+19	99.71%	7.85E+19

F_N accounted for 0.29% and 99.71% of the total energy input, respectively. Therefore, F_R mainly came from the renewable part of the operation cost, followed by hydropower; F_N was mainly derived from lime, followed by the nonrenewable part of the operation cost, and then thermal power. As far as the energy input of the whole system is concerned, phosphate rock accounts for the largest share (48.86%), followed by liquid ammonia (19.32%), the nonrenewable part of operating costs (9.6%), lime (6.04%), sulfur (4.57%), phosphoric acid (4.28%), air (2.60%), coal (1.95%), vanadium catalyst (1.93%); other resources and energy sources contribute to less than 1%.

Compared with Scenario 1, Scenario 2–4 increased the total energy input to varying degrees. The total energy input of scenario 3 was the largest, 3.07 times that of scenario 1. This was mainly due to the large amounts of phosphorus tailings and fertilizer-grade dicalcium phosphate. As shown in Table 1, although the share of R_1 in Scenario 3 decreased by 67.46%, compared with Scenario 1 (Table 1), the share of F_R increased by 29.27 times, and the share of F_N declined by 6.93%, mainly from the input of phosphorus tailings, which are regarded as the main part of F_R because the production rate of phosphate tailings is usually faster than its consumption rate. It was found that Scenario 3 not only recovered solid wastes such as PG and phosphorus tailings but also improved the energy flow structure of the entire system to a certain extent. The total energy input of Scenario 4 increased by 7.05%, compared with Scenario 1, in which the proportions of R_1 and F_R decreased by 6.58% and 0.40%, respectively. The proportion of F_N increased by 0.19% due to the input of lime in the PG manufacturing cement retarder stage. Therefore, this PG reuse method slightly worsens the resource structure of the entire system. Compared with Scenario 1, the total energy input in Scenario 2 increased by 3.15%, mainly from the input of natural gas. Therefore, the proportion of R_1 increased by 17.63%, mainly due to the increase in air input. Whereas the proportion of F_R increased by 12.48%, mainly derived from the increase in hydropower input, and the proportion of F_N decreased by 0.54%. This PG reuse method is beneficial for improving the resource structure of the entire system. Generally, phosphate fertilizer systems depend heavily on nonrenewable resources. Based on the structure of energy flows, the

MAP production stage should concentrate on phosphate rock, liquid ammonia, and operating costs; at the PG disposal stage, Scenario 2 should increase emphasis on natural gas, Scenario 3 should focus on fertilizer-grade dicalcium phosphate, and Scenario 4 should pay more attention to lime. Meanwhile, the resource use of PG generally improved the resource structure of the entire MAP production process, except in Scenario 4.

4.1.2. Pollutant emissions' impacts

As shown in Table 4, Scenario 1 required the most ecological services, followed by Scenarios 2 and 4. In Scenario 1, 99.48% of ecological services were used to dilute water pollutants, and the rest were used to dilute air pollutant emissions. Among these, TP consumes most of the ecological services provided by the aquatic environment, whereas SO_2 utilizes most of the ecological services provided by the atmospheric environment. Similarly, in Scenarios 2–4, 99.40% of the ecological services were used to reduce the concentration of water pollutants (mainly for diluting TP), and the rest were used to dilute air pollutants (mainly for diluting SO_2). However, the resource utilization of PG in Scenarios 2–4 avoids leachate production in the PG slag yard; therefore, the share of ecological services required to dilute water pollutants is reduced. Generally, extra ecological services were reduced by 11.71% after PG reuse than before.

As shown in Table 5, Scenario 1 has the most significant energy loss, followed by Scenario 2, Scenario 3, and Scenario 4. Regarding the contribution of different pollutants to energy loss, dust was the most significant contributor, followed by fluoride and SO_2 emissions, in the four scenarios. Compared with Scenario 1, the share of SO_2 and NO_x in Scenario 2 increased by 2.11% and 100%, respectively, the proportion of dust and solid waste decreased by 62.88% and 100%, and the total energy loss declined by 57.46%; the share of dust and solid waste in Scenario 3 decreased by 62.88% and 100%, respectively, and the total energy loss decreased by 57.66%; the contribution of dust and solid waste in Scenario 4 decreased by 63.68% and 100%, respectively, and the total energy loss declined by 58.27%. The reduction in energy loss in Scenarios 2–4 was derived from the reduction in dust and solid waste

Table 4
Ecological services needed to dilute the air pollutants and water pollutants for the four scenarios.

Item	Acceptable concentration ^a (c)	References	Ecological services (R_2 , sej/yr)			
			Scenario 1	Scenario 2	Scenario 3	Scenario 4
Air pollutants						
Dust	8.00E-08 kg/m ³	b	1.79E+16	6.64E+15	6.64E+15	6.50E+15
NH ₃	2.00E-07 kg/m ³	c	1.02E+14	1.02E+14	1.02E+14	1.02E+14
SO ₂	2.00E-08 kg/m ³	b	2.80E+16	2.86E+16	2.80E+16	2.80E+16
NO _x	5.00E-08 kg/m ³	b	–	9.39E+14	–	–
Sulfuric acid mist	1.00E-07 kg/m ³	c	3.68E+14	3.68E+14	3.68E+14	3.68E+14
Fluoride-containing gas	7.00E-09 kg/m ³	b	1.43E+15	1.43E+15	1.43E+15	1.43E+15
Water pollutants						
COD _{Cr}	1.50E-05 kg/L	d	2.94E+16	2.94E+16	2.94E+16	2.94E+16
SS	2.00E-05 kg/L	e	9.44E+15	9.44E+15	9.44E+15	9.44E+15
Fluoride	1.00E-06 kg/L	d	3.68E+17	9.44E+16	9.44E+16	9.44E+16
TP	2.00E-08 kg/L	d	5.36E+18	4.72E+18	4.72E+18	4.72E+18
TN	2.00E-07 kg/L	d	6.30E+17	6.30E+17	6.30E+17	6.30E+17
NH ₃ -N	1.50E-07 kg/L	d	6.30E+17	6.30E+17	6.30E+17	6.30E+17
Total arsenic	5.00E-08 kg/L	d	3.78E+16	3.78E+16	3.78E+16	3.78E+16
Total ecological services			5.38E+18	4.75E+18	4.75E+18	4.75E+18

Note.

^a To achieve the safest level for human and the environment, the first-grade concentrations in the corresponding environmental quality standards are regarded as the acceptable concentration of the relevant pollutants.

^b Ministry of Ecology and Environment of the People's Republic of China. Ambient air quality standards (GB3095-2012). Available site: http://www.mee.gov.cn/ywgz/fgbz/bz/bzwb/dqhzbz/201203/t20120302_224165.shtml (accessed 09/13/2022, in Chinese).

^c The highest acceptant concentration for harmful material was chosen according to the Hygienic Standards for the Design of Industrial Enterprises (TJ36-79). Available site: <https://www.doc88.com/p-985392093324.html> (accessed 09/13/2022, in Chinese).

^d Ministry of Ecology and Environment of the People's Republic of China. Environmental quality standards for surface water (GB3838-2002). Available site: <http://mee.gov.cn/ywgz/fgbz/bz/bzwb/shjzbz/200206/W02006102750986672057.pdf> (accessed 09/13/2022, in Chinese).

^e Ministry of Ecology and Environment of the People's Republic of China. Integrated Wastewater Discharge Standard (GB 8978-1996). Available site: https://www.mee.gov.cn/ywgz/fgbz/bz/bzwb/shjzbz/swrwpfbz/199801/t19980101_66568.shtml (accessed 09/13/2022, in Chinese).

Table 5

Emergy loss caused by pollutant emissions.

Pollutants' name	Types of damage to human health	DALY ^a	Emergy loss (L, sej/yr)			
		(person·yr/kg)	Scenario 1	Scenario 2	Scenario 3	Scenario 4
Dust	Respiratory disorders	6.29E-04 ^b	4.52E+18	1.68E+18	1.68E+18	1.64E+18
NH ₃	Respiratory disorders	8.50E-05 ^b	8.70E+15	8.70E+15	8.70E+15	8.70E+15
SO ₂	Respiratory disorders	5.46E-05 ^b	1.54E+17	1.57E+17	1.54E+17	1.54E+17
Fluoride-containing gas	Respiratory disorders	5.30E-03 ^b	2.65E+17	2.65E+17	2.65E+17	2.65E+17
NO _x	Respiratory disorders	9.10E-07 ^b	–	2.14E+14	–	–
L _H ^b	–	–	4.94E + 18	2.11E + 18	2.10E + 18	2.07E + 18
PG	–	–	1.78E+16	–	–	–
sludge	–	–	2.33E+12	–	–	–
L _L ^c	–	–	1.78E + 16	–	–	–
Total emergy loss			4.96E + 18	2.11E + 18	2.10E + 18	2.07E + 18

^a These parameters came from Ref. (Huijbregts et al., 2017).^b L_H refers to emergy loss caused by pollutants' harm to human health.^c L_L stands for emergy loss caused by land occupation due to solid waste disposal.

emissions. Generally, the three PG reuse methods cut energy loss by reducing dust emissions and solid waste landfills.

As shown in Tables 6 and 7, the impact of pollutant emissions followed the trend: Scenario 1 > Scenario 2 > Scenarios 3 and 4. Compared with Scenario 1, Scenarios 2–4 reduced the pollutant emissions' impact by 33.72%, 33.76%, and 34.11%, respectively. For the four scenarios, the pollutant emission impact mainly originated from extra ecological services (52.04%, 69.26%, 69.30%, and 69.30% for scenarios 1–4, respectively), followed by energy losses (47.96%, 30.74%, 30.70%, and 30.70% for the four scenarios, respectively). The TP in wastewater should be given the most attention to mitigate the impact of pollutant emissions followed by dust emissions. Therefore, the phosphoric acid production unit should reduce TP discharge into wastewater. Other production units, including the crushing and storage processes of various raw materials, phosphoric acid production, and sulfuric acid production, should further control air emissions from dust, fluorine gas, and SO₂. Generally, PG reuse mitigates the impact of pollutant emissions from the P fertilizer system, mainly because of the apparent reduction in leachate discharge from the slag yard and dust emission reduction from PG storage. This result is consistent with those reported in Ref. (Chernysh et al., 2021).

4.1.3. Indicator values of the four scenarios

As shown in Table 8, the indicator values of EYR followed the trend: Scenario 2 > Scenario 1 > Scenario 4 > Scenario 3. Compared with Scenario 1, the production efficiency of Scenario 2 is increased by 0.51%, which means that the PG reuse in Scenario 2 slightly increased the economic benefits or the competitiveness of the entire system.

Table 6

Statistics of pollutant emissions' impacts of the four scenarios, the shares and change rates of shares.

Item	R ₂	L _H	L _L	Total pollutant emissions' impact
Scenario 1	5.38E+18	4.95E+18	1.78E+16	1.03E+19
Share	52.04%	47.79%	0.17%	100.00%
Scenario 2	4.75E+18	2.11E+18	0.00E+00	6.86E+18
Share	69.26%	30.74%	0.00%	100.00%
Change rate	33.09%	-35.68%	-100.00%	0.00%
Scenario 3	4.75E+18	2.10E+18	0.00E+00	6.85E+18
Share	69.30%	30.70%	0.00%	100.00%
Change rate	33.17%	-35.76%	-100.00%	0.00%
Scenario 4	4.75E+18	2.07E+18	0.00E+00	6.82E+18
Share	69.66%	30.34%	0.00%	100.00%
Change rate	33.86%	-36.51%	-100.00%	0.00%

Note: Change rate = (The share of Scenario i – The share of Scenario 1) × 100%/
The share of Scenario 1. Here i = 2, 3, 4.

However, the market competitiveness of Scenarios 3 and 4 decreased by 1.90% and 0.19%, respectively, compared to that in Scenario 1, mainly because of the slightly increasing share of imported resources for PG reuse in the two scenarios. Generally, the EYR values of the four scenarios are all close to one, indicating that they are highly dependent on imported resources, which leads to low economic efficiency and weak market competitiveness. The three PG reuse methods have little effect on the economic benefits of the entire MAP production process.

Regarding ELR, the indicator values followed the trend: Scenario 4 > Scenario 1 > Scenario 2 > Scenario 3. Compared with Scenario 1, the indicator values of Scenarios 2 and 3 decreased by 15.10% and 70.73%, respectively, whereas those of Scenario 4 increased by 6.58%. In Scenario 3, the proportion of imported renewable energy in the fertilizer-filling material production stage was the largest (mainly from phosphorus tailings), resulting in the most significant reduction in its indicator value compared with Scenario 1. Relative to Scenario 1, the indicator value of Scenario 2 was moderately reduced, mainly because of its rising share of local renewable input (mainly from the air) derived from the production of gypsum powder and gypsum blocks using PG. Compared with Scenario 1, the indicator value of Scenario 4 has increased by 6.58%, mainly because producing cement retarders using PG enhanced the proportion of F_N in the total energy input (mainly from lime). In summary, Scenario 3 significantly reduced the environmental load of MAP production, followed by Scenario 2; however, Scenario 4 moderately increased the environmental load.

The ESI values indicate that Scenario 3 has the highest environmental sustainability level, followed by Scenarios 2, 1, and 4. Compared with Scenario 1, the ESI value of Scenario 3 increases by 2.35 times, mainly because of the lowest environmental load by introducing many phosphorus tailings (here regarded as a renewable resource because of its availability) in the stage of PG resource utilization. Relative to Scenario 1, the ESI value of Scenario 2 increased by 18.38%, which derives from the increased share of renewable resource input in the total energy input by introducing air and hydropower during the resource utilization stage of PG. Compared with Scenario 1, the ESI value of Scenario 4 decreased by 6.35%, mainly because of lime's introduction in the PG resource utilization stage.

Regarding PEI, these indicator values followed the trend of Scenario 1 > Scenario 2 > Scenario 3 > Scenario 4. Compared to that in Scenario 1, PEI values of Scenarios 2, 3, and 4 decreased by 33.72%, 33.76%, and 34.11%, respectively. Therefore, the three types of PG resource utilization methods can reduce the impact of pollutants on human health and the environment, mainly by reducing TP discharge in wastewater and dust emissions in waste gases, compared to that in PG storage.

4.2. CEI values of different scenarios

As illustrated in Table 8, the carbon emission intensity followed the

Table 7

The changes of different kinds of pollutant emissions' impacts in the four scenarios.

Item	Scenario 1	Scenario 2	Change rate	Scenario 3	Change rate	Scenario 4	Change rate
R ₂	5.38E+18	4.75E+18	-11.78%	4.75E+18	-11.79%	4.75E+18	-11.79%
L _H	4.95E+18	2.11E+18	-57.37%	2.10E+18	-57.45%	2.07E+18	-58.17%
L _L	1.78E+16	0.00E+00	-100.00%	0.00E+00	-100.00%	0.00E+00	-100.00%
Total	1.03E+19	6.86E+18	-33.72%	6.85E+18	-33.76%	6.82E+18	-34.11%

Note: Changes rate = (The value of Scenario i - The value of Scenario 1) × 100%/The value of Scenario 1. Here i = 2, 3, 4.

Table 8

Indicator values of the four scenarios.

Item	Scenario 1	Scenario 2	Scenario 3	Scenario 4	Average value
EYR	1.0287	1.0339	1.0092	1.0267	1.0246
Changes rate	-	0.51%	-1.90%	-0.19%	-
ELR	31.4556	26.7072	9.2068	33.5255	25.2238
Changes rate	-	-15.10%	-70.73%	6.58%	-
ESI	0.0327	0.0387	0.1096	0.0306	0.0529
Changes rate	-	18.38%	235.17%	-6.35%	-
PEI	5.7485E+13	3.8102E+13	3.8076E+13	3.7879E+13	4.2885E+13
Changes rate	-	-33.72%	-33.76%	-34.11%	-
CEI	0.3011	0.4046	0.3101	0.3049	0.3302
Changes rate	-	34.38%	3.00%	1.27%	-
SEI	0.5056	0.6720	2.4841	0.7096	1.0928
Changes rate	-	32.90%	391.29%	40.34%	-

Note: Changes rate = (The value of Scenario i - The value of Scenario 1) × 100%/The value of Scenario 1. Here i = 2, 3 and 4.

trend of Scenario 1 (0.3011) < Scenario 4 (0.3049) < Scenario 3 (0.3101) < Scenario 2 (0.4046) in terms of CO₂-eq/t MAP. Compared with Scenario 1, the carbon emission intensity of Scenario 4 increased by 1.27%, owing to an increase in electricity consumption of 26.68%. The diesel and electricity consumption of Scenario 3 increased by 10.00 times and 26.95%, respectively, which resulted in an increase of 3.00% in its carbon emission intensity. The carbon emission intensity of Scenario 2 increased by 34.38% because its electricity consumption was 100.33% higher than that of Scenario 1. The carbon emission intensity of Scenario 2 increased by 34.37% because it consumed extra natural gas for the drying of PG in the rotary kiln, which led to its much higher energy consumption intensity than the other three scenarios. Overall, the three PG resource utilization options raise the carbon emission intensity compared to that in PG storage, mainly related to the increased share of fossil fuels (gas, diesel) and electricity in the total input.

Table 9 shows the contributions of different sources to carbon emissions under the four scenarios. For Scenario 1, the contributions of different sources to carbon emissions followed the trends of fossil fuel combustion > production process > electricity > heat. Specifically, coal contributed the most, followed by the acid decomposition of phosphate rock and electricity. In Scenario 2, the contributions of different sources to carbon emissions followed the trend of fossil fuel combustion > production process > electricity > heat, among which coal was the most significant contributor, followed by natural gas and phosphate rock. In Scenario 3, the contributions of different sources to carbon emissions followed the trend of fossil fuel combustion > production process > electricity > heat, among which coal contributed the most, followed by phosphate rock and electricity. In Scenario 4, the contributions of different sources to carbon emissions followed the trend of fossil fuel combustion > production process > electricity > heat, among which coal contributed the most, followed by phosphate rock and electricity. In the four scenarios, carbon emissions mainly come from the combustion of fossil fuels (such as coal and natural gas) and the decomposition of phosphate rock. Therefore, to reduce the carbon emissions of the MAP production system, special attention should be paid to the structure of the energy sources and raw materials, in addition to their efficiency.

4.3. SEI of different scenarios

As shown in **Table 8**, Scenario 3 exhibited the best synergistic effect

Table 9

Carbon emission statistics of the four scenarios.

Item	Source	CE (t CO ₂ /t MAP)	Share (%)
Scenario 1	Fossil fuel combustion	2.29E-01	76.01%
	Coal	2.28E-01	75.84%
	Diesel	5.17E-04	0.17%
	Production process	4.53E-02	15.04%
	Decomposition of phosphate rock	4.53E-02	15.04%
	Electric power	1.43E-02	4.76%
	Electricity	1.43E-02	4.76%
	Heating power	1.26E-02	4.19%
	Steam	1.26E-02	4.19%
	Total	3.01E-01	100.00%
Scenario 2	Fossil fuel combustion	3.18E-01	78.59%
	Coal	2.28E-01	56.43%
	Diesel	5.17E-04	0.13%
	Natural gas	8.91E-02	22.03%
	Production process	4.53E-02	11.19%
	Decomposition of phosphate rock	4.53E-02	11.19%
	Electric power	2.87E-02	7.10%
	Electricity	2.87E-02	7.10%
	Heating power	1.26E-02	3.12%
	Steam	1.26E-02	3.12%
Scenario 3	Total	4.05E-01	100.00%
	Fossil fuel combustion	2.34E-01	75.46%
	Coal	2.28E-01	73.63%
	Diesel	5.68E-03	1.83%
	Production process	4.53E-02	14.60%
	Decomposition of phosphate rock	4.53E-02	14.60%
	Electric power	1.82E-02	5.87%
	Electricity	1.82E-02	5.87%
	Heating power	1.26E-02	4.07%
	Steam	1.26E-02	4.07%
Scenario 4	Total	3.10E-01	100.00%
	Fossil fuel combustion	2.29E-01	75.06%
	Coal	2.28E-01	74.89%
	Diesel	5.17E-04	0.17%
	Production process	4.53E-02	14.85%
	Decomposition of phosphate rock	4.53E-02	14.85%
	Electric power	1.82E-02	5.96%
	Electricity	1.82E-02	5.96%
	Heating power	1.26E-02	4.14%
	Steam	1.26E-02	4.14%

(2.4841), followed by Scenarios 4 (0.7096), Scenario 2 (0.6720), and Scenario 1 (0.5056). Compared with Scenario 1, the SEI value of Scenario 3 increased by 3.91 times because it had a much higher ESI value and lower PEI and CEI values than the average levels of the four scenarios, indicating that this scenario had the highest synergistic effect among its resource efficiency and structure, pollution control, and carbon emission reduction. Relative to Scenario 1, the SEI value of Scenario 4 increased by 40.34%, mainly because of its lowest values of PEI and CEI among the four scenarios, which surpassed the adverse effect of its lowest value of ESI. Compared with Scenario 1, the SEI value of Scenario 2 increased by 32.90%, mainly derived from its enhanced ESI value and reduced PEI value, which offset the adverse impact of its increasing CEI value. The SEI value of Scenario 1 was the lowest among the four scenarios because the adverse effects from its low ESI value and high PEI value exceeded the positive contribution from its lowest CEI value in the four scenarios. Relative to PG storage Generally, the three PG reuse options improved the synergistic effects of the MPA production system to a certain degree.

The results from the three types of performance indicators conflict with each other to different degrees, which could confuse decision-makers. However, performance indicators from diverse angles should be considered simultaneously in practical decision-making to promote harmony or oneness of the system under study for sustainable development (Birkin et al., 2021). Therefore, the results from these single indicators should be integrated into an overall picture convenient for comprehensive decision-making. The results from a single indicator can provide detailed information on specific aspects for implementing targeted measures in the future. Consequently, these single indicators and the integrated index can form a set of valuable tools for systematic policymaking.

4.4. Factors affecting SEI

Table 10 shows the impact of various single indicators on the SEI. In Scenario 1, the positive contribution to SEI was from the CEI, and the most considerable adverse impact was mainly from the ESI, followed by the PEI. In Scenario 2, the positive contribution to SEI was from PEI, and the negative impact was mainly from ESI, followed by CEI. In Scenario 3, ESI contributed the most to SEI, followed by PEI and CEI, showing an excellent synergistic effect among the three performance indicators. In Scenario 4, the negative impact comes from ESI, and the positive impacts are mainly from PEI, followed by CEI. Therefore, the environmental sustainability and pollution emissions' impacts should be emphasized for Scenario 1, the environmental sustainability and carbon emission intensity should be considered for Scenario 2, the carbon emission intensity could be moderately reduced in Scenario 3 (higher than Scenario 1), and the environmental sustainability should be significantly improved in Scenario 4.

Finally, the main findings are as follows: Scenario 3 has the highest level of environmental sustainability, Scenario 4 has the lowest pollutant emissions' impact intensity, and the carbon emission intensity of Scenario 1 is the lowest. Generally, Scenario 3 had the best synergistic effect due to the promotion of efficient life cycle P management (Liu et al., 2016), which can also be supported by the research of Liu et al.

Table 10
Indicator values of the SDI and ID for the four scenarios.

Item	SEI	ID ₁	ID ₂	ID ₃
Scenario 1	0.5056	-0.3820	-0.2540	0.0966
Scenario 2	0.6720	-0.2684	0.1255	-0.1840
Scenario 3	2.4841	1.0715	0.1263	0.0647
Scenario 4	0.7096	-0.4212	0.1322	0.0829

Note: SEI: Synergistic effect index. ID_i refers to the degree of influence of the i-th indicator on the SEI. Therein, ID₁, ID₂, and ID₃ refers to the influence degree of ESI, PEI, and CEI on the SEI, respectively.

(2023) based on comparison of decreased per capita phosphate consumption from three recycling methods (waste as fertilizer, waste as feed, and waste as industrial material). Therefore, phosphate fertilizer manufacturers should choose reasonable resource utilization ways of PG, such as producing fertilizer filling materials using PG. However, different PG resource utilization ways can provide various products to meet specific market demands. Therefore, the following issues should be further addressed, including optimizing the energy structure (especially coal) of Scenario 3 to reduce carbon emission intensity further, improving the environmental sustainability of Scenario 4 by adjusting the resource structure (mainly lime), and promoting the environmental sustainability and reducing carbon emission intensity of Scenario 2 by improving its resource structure and energy mix. Since the pollution emissions of the four scenarios mainly come from TP discharge in wastewater and dust and SO₂ emissions, relevant measures against these pollutants should also be strengthened in the future.

5. Discussion

5.1. Sensitivity analysis

Factors such as changes in some primary data caused by data collection methods, adjustment of process parameters, and mismatches in some unit energy values may affect the energy evaluation results to varying degrees. Sensitivity analysis was performed to evaluate the influence of the main input parameters on the main energy-based indicator results. Based on the energy flow structure, the main input parameters in the four scenarios were used to implement the sensitivity analysis. One of these input values is assumed to change between -10% and 10%, whereas the others remain unchanged. The current energy indicator values were used as reference values to compare the changes in relevant indicator values, as shown in SM-10.1–10.4. It can be found (SM-10.1) that when phosphate rock, liquid ammonia, and operating costs change between -10% and ~10%, all indicator values in Scenario 1 fluctuate between -5.26% and ~5.87%. The results from SM-10.2 show that when input values of phosphate rock, liquid ammonia, and operating costs alter between -10% and ~10%, all indicator values in Scenario 2 change between -5.15% and ~5.74%. The results from SM-10.3 illustrate that when input values of phosphate rock, fertilizer-grade dicalcium phosphate, and phosphate tailings change between -10% and 10%, all indicator values in scenario 3 fluctuate between -8.94% and 9.82%. When input values of phosphate rock, liquid ammonia, and operating costs change between -10% and ~10%, all indicator values in Scenario 4 range from -5.03% to 5.44% (SM-10.4). Generally, when these input values vary between -10% and ~10%, change rates of the energy-based indicator values in the four scenarios fall into the scope of -10% and ~10%. Therefore, changes in the main input values have limited impacts on energy-based indicator values; thus, the evaluation results can act as references for subsequent decision-making.

Meanwhile, phosphate rock has the most significant influence on ESI, followed by ELR; the phosphorus tailings have the most significant impact on ELR, followed by ESI. Therefore, the data quality of these two input parameters should be emphasized in future studies. In addition, it should be noted that the impact of emissions may be affected to some extent by ignoring R₃ caused by environmental emissions and the potential dangers of trace metals and natural radioactive substances during PG storage. As for the effect of neglect of ecological losses, the work of Liu et al. (2013) showed that the impact of R₃ on total emissions ranged between 2.48% and 10.38%. Therefore, generally neglecting R₃ has a limited effect on the conclusions.

For carbon emissions, the primary data are from our investigation, related emission parameters are cited from authoritative references, and all of these ensure the reliability of the results. Related economic evaluations were not considered because of the unavailability of primary data. However, these issues require further investigation.

5.2. Policy suggestions

Relative to Scenario 1, although Scenarios 2–4 enhanced the synergistic effect of the holistic MAP production process to different degrees, the three PG resource utilization methods also incurred some new issues that should be emphasized. Scenario 2 had the most significant CEI value of the four scenarios, mainly due to rapidly increasing electricity consumption, followed by fossil fuel use relative to Scenario 1. Scenario 3 had a higher CEI value than Scenario 1 because of the moderately increased electricity consumption. Scenario 4 has the lowest ESI value of the four scenarios, mainly rooted in its moderately declining share of renewable inputs (especially the decreasing share of local renewable input) and a slightly rising share of nonrenewable inputs (mainly caused by lime). Therefore, these PG reuse methods cannot ultimately realize a synergistic effect between waste reduction and carbon emission reduction, mainly because of the worsening structure of resources and energy sources. The following are the suggestions to address these issues.

Firstly, improving the energy mix for cutting carbon emissions. Compared with Scenario 1, the three PG resource utilization methods increased the carbon emission intensity to different degrees. Targeted countermeasures should be implemented to reduce additional carbon emissions from PG reuse. The additional carbon emissions in Scenario 2 were mainly derived from natural gas combustion for the drying of PG in the rotary kiln, which can be mitigated by replacing natural gas with waste heat from the MPA production process. This measure can reduce imports from fossil energy sources (Liu et al., 2015). For example, the outlet gas temperature of a sulfur incinerator can reach about 1020 °C. In addition to being used for power generation, excess heat energy can also be used for PG drying pretreatment. Artificial intelligence could be introduced in production management. For example, an instrument developed by the Lubei Group (Bao, 2017) can provide detailed information for the automatic control of a rotary kiln through automatic sampling and rapid analysis of high-temperature kiln gas to save energy and reduce emissions. Advanced grinding equipment can be considered to reduce electric power consumption in production while reducing carbon dioxide emissions. For example, vertical and roller mills can save about 30% of electricity consumption relative to ball mills (Ali et al., 2011). The increased carbon emissions in Scenario 3 are mainly rooted in diesel and electricity consumption, which can be cut through adjustment of the fuel structure using biofuels such as biodiesel and bioethanol, and recovery and utilization of exhaust gas energy to reduce diesel use. A diesel engine can realize the recovery and utilization of exhaust gas energy by increasing the intake pressure with exhaust gas turbocharging technology, which can improve thermal efficiency by optimizing the automatic control of the circulating fuel supply (Yang et al., 2022), and introducing more clean and/or renewable electricity sources, such as wind, solar, and bioenergy. The extra carbon emissions in Scenario 4 mainly come from enhanced electricity consumption; therefore, this scenario could improve its electricity mix by taking measure proposed for Scenario 3.

The second suggestion is adjusting the resource structure to raise sustainability. Compared with the PG storage in Scenario 1, the manufacturing of cement retarders in Scenario 4 reduced the environmental sustainability of the entire production process owing to the worsening resource structure, mainly caused by the introduction of lime. The PG/lime ratio can be optimized to ensure product quality to address this issue. Li and Wei (2019) found that carbide slag can be used as a modifier in place of lime, and adding 0.3% carbide slag to PG can effectively remove soluble phosphorus and fluorine after a chemical reaction of 2 h. The modified PG can be used as a cement retarder to increase cement strength, extend its service life, and reduce costs. Thus, this technology can achieve waste control and has potential environmental and economic advantages.

Thirdly, some standard measures for the four scenarios can be considered, including fully utilizing the local discarded hydroelectricity in the wet season. Hydroelectric resources are abundant in Hubei

Province, China. However, a large amount of hydroelectricity is discarded because the sluice gate opens during the wet season. Thus, the MAP production enterprise can utilize discarded electricity to improve its electricity mix and reduce the energy loss of pipelines and heat utilization equipment. Related measures include optimizing the network configuration of natural gas and gas supply pipelines by designing a reasonable pipeline diameter, reducing the leakage rate, raising pump efficiency, keeping heat utilization equipment working in a good state of anti-corrosion and heat insulation, and increasing the energy efficiency of kilns and hot blast stoves. Related measures include the application of advanced kilns, strengthening the sealing performance of hot-blast stoves, improving the stability of the coal feeding system, and strengthening pollutant control.

Regarding the impact of pollution emissions, those pollutants, including dust, SO₂, and TP, should be effectively treated using advanced technologies. For example, Peng et al. (2022) developed an integrated high-efficiency dust removal, desulfurization, and denitrification treatment process that can reduce investment in enterprises. In addition, acidic PG sewage can replace part of the sulfuric acid, acting as a pH adjuster in phosphate rock flotation (Zhang, 2021), or partially replace fresh water to realize the resource utilization of wastewater containing phosphorus. Advanced technologies can be used to reduce pollutant emissions from PG storage. Liu et al. (2022) proved that using γ-Al₂O₃ could be an efficient technology for large-scale stockpiled PG remediation through the role of aluminum-containing assemblages in the retention of fluorine, phosphorus, and sulfate.

Finally, strengthening the life cycle management of PG is necessary. Currently, the phosphate fertilizer production system and PG reuse are mostly separate in China, which is not conducive to optimizing their overall performance. Therefore, enterprises should be encouraged to integrate these two systems into one integrated system to improve their resources and energy efficiency (Yang, 2021). It is suggested that the entire life cycle investigation, consisting of domestic phosphate rock mining and dressing, phosphate fertilizer production, and PG resource utilization, a solution for effective PG management from the source to accelerate the sustainable utilization of PG in China's phosphorus chemical industry should be explored. Currently, PG utilization in China is mainly in a state of primary processing and utilization, and its comprehensive performance is relatively low. The Chinese government should promote the research and development of PG resource utilization in new functional coatings, extraction of rare earth, high-end building materials, etc., to extend large-scale, multi-channel utilization of PG. The related pollution taxes and effective subsidy policies should also be improved to promote PG waste recycling and reuse in enterprises and related stakeholders (Xu et al., 2019).

6. Conclusion

This study proposes a comprehensive indicator system to investigate the effects of different PG disposal methods on the environmental performance of an integrated system composed of MAP production and PG disposal, from environmental sustainability, pollutant emission impacts, carbon emission intensity, and their synergistic effects. The main conclusions are summarized as follows: Relative to Scenario 1, the three PG resource utilization methods enhance the synergistic effect of the integrated system to different degrees by increasing the energy sustainability and/or reducing the impact of pollutant emissions. Comparatively speaking, Scenario 3 has the best synergistic effect, followed by Scenarios 4 and 2, and Scenario 1 ranked the last. These PG reuse methods enhance carbon emission intensities due to increasing fossil energy use. Based on nonrenewable resources/energy source inputs, PG reuse methods could cause conflict between waste reduction and carbon emission reduction. Clean and/or renewable resources and energy sources should first be chosen as supplementary raw materials and as a driving force for controlling extra carbon emissions to promote the synergistic effect of PG resource utilization. This study contributes to

environmental management by constructing an integrated approach to thoroughly investigate the environmental performance of an integrated system consisting of phosphate fertilizer production and PG disposal. Therefore, we provide targeted decision-making information for phosphate fertilizer production in China.

CRediT authorship contribution statement

Zeying Wang: Raw data collection, Methodology, Writing – original draft. **Xiaohan Ma:** Check of Raw data and, Methodology, and, revision of Original draft, Writing – original draft. **Hengyu Pan:** Preparation of raw data, Methodology. **Xiangdong Yang:** Check of Raw data and, Methodology, and, revision of Original draft, Writing – original draft. **Xiaohong Zhang:** Conceptualization, emery analysis, Formal analysis, the indicator system construction, Data curation, manuscript revision, Resources, Funding acquisition. **Yanfeng Lyu:** improvement of, Methodology, and, revision of Original draft, Writing – original draft. **Wenjie Liao:** improvement of, Methodology, and, revision of Original draft, Writing – original draft. **Wei Shui:** improvement of, Methodology, and, revision of Original draft, Writing – original draft. **Jun Wu:** improvement of fertilization schemes. **Min Xu:** revision of Original draft, Writing – original draft. **Yanzong Zhang:** Supervision, and, management of the projects. **Shirong Zhang:** Check of, Methodology, Software. **Yinlong Xiao:** Check of Raw data. **Hongbing Luo:** Software.

Declaration of competing interest

The authors declare that they have no known competing financial interests or personal relationships that could have appeared to influence the work reported in this paper.

Data availability

We have provided related basic data in the supplementary materials.

Acknowledgments

This study was supported by the Dual Support Plan of Sichuan Agricultural University (03570312, 03571248, 03571906, and 03572533).

Appendix A. Supplementary data

Supplementary data to this article can be found online at <https://doi.org/10.1016/j.jclepro.2023.137248>.

References

- Alcordo, L.S., Rechcigl, J.E., 1993. Phosphogypsum in agriculture: a review. *Adv. Agron.* 49, 55–118. Academic Press.
- Ali, M., Marvuglia, A., Geng, Y., Chaudhry, N., Khokhar, S., 2018. Emery based carbon footprinting of household solid waste management scenarios in Pakistan. *Resour. Conserv. Recycl.* 131, 283–296.
- Ali, M.B., Saidur, R., Hossain, M.S., 2011. A review on emission analysis in cement industries. *Renew. Sustain. Energy Rev.* 15, 2252–2261.
- Bao, S.T., 2017. New technology development of producing sulphuric acid and cement from industrial by-product gypsum. *Sulphuric Acid Ind* 2, 51–56 (in Chinese).
- Birkin, F., Margerison, J., Monkhouse, L., 2021. Chinese environmental accountability: ancient beliefs, science and sustainability. *Resources, Environment and Sustainability* 3, 100017.
- Björklund, J., Geber, U., Rydberg, T., 2001. Emery analysis of municipal wastewater treatment and generation of electricity by digestion of sewage sludge. *Resour. Conserv. Recycl.* 31, 293–316.
- Brown, M.T., Campbell, D.E., Vilbiss, C.D., Ulgiati, S., 2016. The geobiosphere emery baseline: a synthesis. *Ecol. Model.* 339, 92–95.
- Brown, M.T., Ulgiati, S., 2010. Updated evaluation of exergy and emery driving the geobiosphere: a review and refinement of the emery baseline. *Ecol. Model.* 221, 2501–2508.
- Brown, M.T., Ulgiati, S., 2016. Emery assessment of global renewable sources. *Ecol. Model.* 339, 148–156.
- Cai, W., Liu, C.H., Zhang, C.X., Ma, M.D., Rao, W.Z., Li, W.Y., He, K., Gao, M.d., 2018. Developing the ecological compensation criterion of industrial solid waste based on emery for sustainable development. *Energy* 157, 940–948.
- Campbell, D.E., 1998. Emery analysis of human carrying capacity and regional sustainability: an example using the State of Maine. *Environ. Monit. Assess.* 51, 531–569.
- Canut, M.M.C., Jacomino, V.M.F., Bråtevit, K., Gomes, A.M., Yoshida, M.I., 2008. Microstructural analyses of phosphogypsum generated by Brazilian fertilizer industries. *Mater. Char.* 59, 365–373.
- Cao, J., Wang, Z., Ma, X., Yang, X., Zhang, X., Pan, H., Wu, J., Xu, M., Lin, L., Zhang, Y., Xiao, Y., Luo, H., 2022. Promoting coordinative development of phosphogypsum resources reuse through a novel integrated approach: a case study from China. *J. Clean. Prod.* 374, 134078.
- Chen, S.R., Dong, G.X., Zhang, F.Y., Li, Y.L., Zhou, M., Ma, G.W., He, L.H., Lin, L.Y., 2022. Surface water quality and correlation analysis of the yangtze river economic belt during the 13th five-year plan period. *J. Environ. Eng. Technol.* 12, 361–369 (in Chinese).
- Chen, Y.T., Hu, S.Y., Chen, D.J., Zhai, H.X., Bao, S.T., Lv, T.B., 2019. An evaluation method of green development for chemical enterprises. *Sustainability* 11, 22.
- Chernysh, Y., Yakhnenko, O., Chubur, V., Roubík, H., 2021. Phosphogypsum recycling: a review of environmental issues, current trends, and prospects. *Appl. Sci.* 11 (4), 1575.
- Contreras, M., Perez-Lopez, R., Gazquez, M.J., Morales-Florez, V., Santos, A., Esquivias, L., Bolivar, J.P., 2015. Fractionation and fluxes of metals and radionuclides during the recycling process of phosphogypsum wastes applied to mineral CO₂ sequestration. *Waste Manage. (Tucson, Ariz.)* 45, 412–419.
- Cui, R., Bai, H., Gao, Y., Xiu, X., 2022a. Current situation of comprehensive utilization of phosphogypsum and its development trend of 14th Five-Year Plan. *Inorg. Chem. Ind* 54, 1–4 (in Chinese).
- Cui, Y., Chang, L.S., Yang, S., Yu, X.K., Cao, Y.M., Wu, J., 2022b. A novel dynamic business model to quantify the effects of policy intervention on solid waste recycling industry: a case study on phosphogypsum recycling in Yichang, China. *J. Clean. Prod.* 355, 131779.
- Da Silva, G.A., Kulay, L.A., 2005. Environmental performance comparison of wet and thermal routes for phosphate fertilizer production using LCA – a Brazilian experience. *J. Clean. Prod.* 13, 1321–1325.
- Delgado, A., Uceda, I., Andreu, L., Kassem, S., Del Campillo, M.C., 2002. Fertilizer phosphorus recovery from gypsum-amended, reclaimed calcareous marsh soils. *Arid Land Res. Manag.* 16, 319–334.
- Dijkstra, J.J., Meeussen, J.C.L., Comans, R.N.J., 2004. Leaching of heavy metals from contaminated soils: an experimental and modeling study. *Environ. Sci. Technol.* 38, 4390–4395.
- Dong, L., Miao, G.Y., Wen, W.G., 2021. China's carbon neutrality policy: objectives, impacts and paths. *East Asian Policy* 1, 5–18.
- Du, J.X., Han, T.F., Qu, X.L., Ma, C.B., Liu, K.L., Huang, J., Shen, Z., Zhang, L., Liu, L.S., Xie, J.H., Zhang, H.M., 2022. Spatial-temporal evolution characteristics and driving factors of partial phosphorus productivity in major grain crops in China. *J. Plant Nutr. Fert.* 28, 191–204 (in Chinese).
- Ecoinvent center, 2010. Swiss center for life cycle inventories. <https://ecoinvent.org/the-ecoinvent-database/>.
- Gao, W.M., Ran, J., Zhu, Q.H., 2022. Policy interpretation and research progress of resource utilization of phosphogypsum in China. *Ind. Miner. Process.* 51, 48–53 (in Chinese).
- Huang, L.H., Liu, Y., Ferreira, J.F.S., Wang, M.M., Na, J., Huang, J.X., Liang, Z.W., 2022. Long-term combined effects of tillage and rice cultivation with phosphogypsum or farmyard manure on the concentration of salts, minerals, and heavy metals of saline-sodic paddy fields in Northeast China. *Soil Tillage Res.* 215, 105222.
- Huijbregts, M.A.J., Steinmann, Z.J.N., Elshout, P.M.F., Stam, G., Verones, F., Vieira, M., Zijp, M., Hollander, A., Zel'm, R.V., 2017. ReCiPe2016: a harmonised life cycle impact assessment method at midpoint and endpoint level. *Int. J. Life Cycle Assess.* 22, 138–147.
- Jia, X.T., Liu, J.D., Xu, T.F., 2019. Application status and development of exterior wall insulation materials. *Construction Safety* 34 (7), 74–77 (in Chinese).
- Kulczycka, J., Kowalski, Z., Smol, M., Wirth, H., 2016. Evaluation of the recovery of rare earth elements (REE) from phosphogypsum waste – case study of the wizów chemical plant (Poland). *J. Clean. Prod.* 113, 345–354.
- Li, B., Wei, S., 2019. Modification of phosphogypsum cement retarder by carbide slag. *Inorg. Chem. Ind.* 51, 74–76 (in Chinese).
- Liu, G.Y., Hao, Y., Dong, L., Yang, Z.F., Zhang, Y., Ulgiati, S., 2017. An emery-LCA analysis of municipal solid waste management. *Resour. Conserv. Recycl.* 120, 131–143.
- Liu, G., Yang, Z., Chen, B., Zhang, Y., Su, M., Zhang, L., 2013. Emery evaluation of the urban solid waste handling in liaoning province, China. *Energies* 6, 5486–5506.
- Liu, G.Y., Yang, Z.F., Chen, B., Zhang, J.R., Liu, X.Y., Zhang, Y., Su, M.R., Ulgiati, S., 2015. Scenarios for sewage sludge reduction and reuse in clinker production towards regional eco-industrial development: a comparative emery-based assessment. *J. Clean. Prod.* 103, 371–383.
- Liu, X., Sheng, H., Jiang, S., Yuan, Z., Zhang, C., Elser, J.J., 2016. Intensification of phosphorus cycling in China since the 1600s. *Proc. Natl. Acad. Sci. U. S. A* 113 (10), 2609–2614.
- Liu, X., Yuan, Z., Liu, X., Zhang, Y., Hua, H., Jiang, S., 2020. Historic trends and future prospects of waste generation and recycling in China's phosphorus cycle. *Environ. Sci. Technol.* 54, 5131–5139.
- Liu, X., Zhang, Y., Cheng, M., Jiang, S., Yuan, Z., 2023. Recycling phosphorus from waste in China: recycling methods and their environmental and resource consequences. *Resour. Conserv. Recycl.* 188, 106669.

- Liu, Y., Chen, Q., Dalconi, M.C., Molinari, S., Valentini, L., Wang, Y., Sun, S., Wang, P., Artioli, G., 2022. Enhancing the sustainable immobilization of phosphogypsum by cemented paste backfill with the activation of γ -Al₂O₃. *Construct. Build. Mater.* 347, 128624.
- Lou, Y.X., Yang, Z., Xu, H.G., 2019. Manufacturing and micro-structure of high strength desulfurization gypsum blocks. *J. Liaoning Norm. Univ., Nat. Sci. Ed.* 42, 83–87 (in Chinese).
- Lu, Y., Chen, B., 2014. Urban studies based on energy—A review in perspective of causality. *Energy Proc.* 61, 2546–2549.
- Ma, S.J., Luo, Z.B., Hu, S.Y., Chen, D.J., 2018. Promoting information technology for the sustainable development of the phosphate fertilizer industry: a case study of Guizhou Province, China. *R. Soc. Open Sci.* 5, 181160.
- Mohammed, F., Biswas, W.K., Yao, H., Tadé, M., 2018. Sustainability assessment of symbiotic processes for the reuse of phosphogypsum. *J. Clean. Prod.* 188, 497–507.
- National Bureau of statistics of China (NBSC), 2015. National data 2016. [DB/OL] Available site. <https://data.stats.gov.cn/search.htm?s=GDP>. (Accessed 16 June 2022).
- National Bureau of statistics of China (NBSC), 2020. National data 2021. [DB/OL] Available site. <https://data.stats.gov.cn/search.htm?s=GDP>. (Accessed 16 June 2022).
- National environmental accounting database (NEAD). NEAD data by country, China. Available site. <http://www.emergy-nead.com/country/data->. (Accessed 16 June 2022).
- Odum, H.T., 1988. Self-organization, transformity, and information. *Science* 242, 1132–1139.
- Odum, H.T., 1996. Environmental Accounting: Energy and Environmental Decision Making. John Wiley and Sons, New York, USA.
- Odum, H.T., 2000. Handbook of Energy Evaluation (Folio #2): a Compendium of Data for Energy Computation Issued in a Series of Folios. Center for Environmental Policy, Environmental Engineering Sciences, University of Florida, Gainesville, FL.
- Ogunmoroti, A., Liu, M., Li, M., Liu, W., 2022. Unraveling the environmental impact of current and future food waste and its management in Chinese provinces. *Resources, Environment and Sustainability* 9, 100064.
- Ou, Z.B., Yang, W.J., He, B.B., 2021. The general introduction of phosphogypsum comprehensive utilization technology in China. *Yunnan Chem. Technol.* 48 (11), 6–9 (in Chinese).
- Pan, H., Zheng, X., Tian, X., Geng, Y., Zhang, X., Xiao, S., Gao, Z., Yang, Y., Liu, X., Li, L., Huang, C., Deng, S., Liu, Q., 2022. Toward sustainable crop production in China: a co-benefits evaluation. *J. Clean. Prod.* 361, 132285.
- Peng, J.X., Li, D.L., Sheng, P.F., Zheng, X.J., 2022. Research and application of efficient dust removal, desulfurization and denitrification treatment machine processing technology in the field of environmental protection. *Coal Process. Compr. Util.* 8, 7–80 (in Chinese).
- Pradel, M., Lippi, M., Daumer, M.L., Aissani, L., 2020. Environmental performances of production and land application of sludge-based phosphate fertilizers—a life cycle assessment case study. *Environ. Sci. Pollut. Res.* 27, 2054–2070.
- Salemdeeb, R., Saint, R., Clark, W., Lenaghan, M., Pratt, K., Millar, F., 2021. A pragmatic and industry-oriented framework for data quality assessment of environmental footprint tools. *Resources, Environment and Sustainability* 3, 100019.
- Shao, L., Chen, G.Q., 2016. Renewability assessment of a production system: based on embodied energy as energy. *Renew. Sustain. Energy Rev.* 57, 380–392.
- Takahashi, T., Ikeda, Y., Nakamura, H., Nanzyo, M., 2006. Efficiency of gypsum application to acid Andosols estimated using aluminum release rates and plant root growth. *J. Soil Sci. Plant Nutr.* 52, 584–592.
- Tang, Z., Lei, T., Yu, J., Shainberg, I., Mamedov, A.I., Ben-Hur, M., Levy, G.J., 2006. Runoff and interrill erosion in sodic soils treated with dry PAM and phosphogypsum. *Soil Sci. Soc. Am. J.* 70, 679–690.
- Tayibi, H., Choura, M., López, F.A., Alguacil, F.J., López-Delgado, A., 2009. Environmental impact and management of phosphogypsum. *J. Environ. Manag.* 90, 2377–2386.
- Tsioka, M., Voudrias, E.A., 2020. Comparison of alternative management methods for phosphogypsum waste using life cycle analysis. *J. Clean. Prod.* 266, 121386.
- Ukidwe, N., Bakshi, B., 2004. Thermodynamic accounting of ecosystem contribution to economic sectors with application to 1992 U.S. economy. *Environ. Sci. Technol.* 38, 4810–4827.
- Ulgiati, S., Brown, M.T., 1998. Monitoring patterns of sustainability in natural and man-made ecosystems. *Ecol. Model.* 108, 23–36.
- Ulgiati, S., Brown, M.T., 2002. Quantifying the environmental support for dilution and abatement of process emissions: the case of electricity production. *J. Clean. Prod.* 10, 335–348.
- Valkov, A.V., Andreev, V.A., Anufrieva, A.V., Makaseev, Y.N., Bezrukova, S.A., Demyanenko, N.V., 2014. Phosphogypsum technology with the extraction of valuable components. *Procedia Chem.* 11, 176–181.
- Wang, J.N., Yu, F., Cao, D., 2006. Study report 2004 for green national economic accounting. China population. *Resour. Environ.* 16 (6), 11–17 (in Chinese).
- Wang, X.L., Li, Z.J., Long, P., Yan, L.L., Gao, W.S., Chen, Y.Q., Sui, P., 2017. Sustainability evaluation of recycling in agricultural systems by energy accounting. *Resour. Conserv. Recycl.* 117, 114–124.
- Wang, Y., Fang, J.W., Li, B., 2021a. Production and developing trends of phosphate and compound fertilizer industry in China in 2020. *Phosphate Compd. Fert.* 36, 1–8 (in Chinese).
- Wang, Y., Yuan, Z., Tang, Y., 2021b. Enhancing food security and environmental sustainability: a critical review of food loss and waste management. *Resources, Environment and Sustainability* 4, 100023.
- Wang, Y.Q., Zhang, X.H., Liao, W.J., Wu, J., Yang, X.D., Shui, W., Deng, S.H., Zhang, Y.Z., Lin, L.L., Xiao, Y.L., Yu, X.Y., Peng, H., 2018. Investigating impact of waste reuse on the sustainability of municipal solid waste (MSW) incineration industry using energy approach: a case study from Sichuan province, China. *Waste Manag.* 77, 252–267.
- Wei, Z.Q., Zhang, Q., Li, X.B., 2021. Crystallization kinetics of α -hemihydrate gypsum prepared by hydrothermal method in atmospheric salt solution medium. *Crystals* 11, 843.
- Wu, F.H., Liu, X.X., Wang, C.P., Qu, G.F., Liu, L.L., Chen, B.J., Zhao, C.Y., Liu, S., Li, J.Y., 2022. New dawn of solid waste resource treatment: preparation of high-performance building materials from waste-gypsum by mechanical technology. *Construct. Build. Mater.* 318, 126204.
- Xiao, X.D., 2021. Study on Life Cycle Carbon Emission and Life Cycle Cost of Green Buildings. Master's Theses. Beijing Jiaotong University (In Chinese).
- Xu, J.J., Zhang, N.M., 2017. Research progress for applications of phosphogypsum in agriculture. *Phosphate Compd. Fert.* 32, 34–38 (In Chinese).
- Xu, J.P., Fan, L.R., Xie, Y.C., Wu, G., 2019. Recycling-equilibrium strategy for phosphogypsum pollution control in phosphate fertilizer plants. *J. Clean. Prod.* 215, 175–197.
- Yang, C.B., Chen, H.L., Wei, W., 2022a. Research on the development of synergia energy conservation technology of reciprocating internal combustion engine. *Intern. Combust. Eng. Parts* (13), 106–109 (in Chinese).
- Yang, L., Ren, H., Wang, M., Liu, N., Mi, Z., 2022b. Assessment of eco-environment impact and driving factors of resident consumption: taking Jiangsu Province, China as an example. *Resources, Environment and Sustainability* 8, 100057.
- Yang, L., Zhang, Y.S., Yan, Y., 2016. Utilization of original phosphogypsum as raw material for the preparation of self-leveling mortar. *J. Clean. Prod.* 127, 204–213.
- Yang, Z., 2021. Development trend of gypsum building materials under the situation of carbon peak and carbon neutralization. *Sulphuric Acid Industry* (8), 1–4 (in Chinese).
- Yuan, Z., Jiang, S., Sheng, H., Liu, X., Hua, H., Liu, X., Zhang, Y., 2018. Human perturbation of the global phosphorus cycle: changes and consequences. *Environ. Sci. Technol.* 52, 2438–2450.
- Zhang, B., Hou, C., Tang, J., Wang, G., 2011. To develop low-carbon and environmental protection phosphate industry by way of saving energy and reducing discharge. *Chemical fertilizer industry* 38 (3), 1–5, 9. (in Chinese).
- Zhang, B., 2021. Experimental study on substitution of acid wastewater from phosphogypsum slag field for sulfuric acid in flotation of phosphate ore. *Guangzhou Chem. Ind.* 49, 114–117 (in Chinese).
- Zhang, F., 2016. Life-cycle Assessment of Ammonium Phosphate Production in China. Shandong University, Jinan, China. p. 6 (in Chinese).
- Zhang, F.F., Wang, Q.S., Hong, J.L., Chen, W., Qi, C.C., Ye, L.P., 2017. Life cycle assessment of diammonium- and monoammonium-phosphate fertilizer production in China. *J. Clean. Prod.* 141, 1087–1094.
- Zhang, W.F., Ma, W.Q., Ji, Y.X., Fan, M.S., Oenema, O., Zhang, F.S., 2008. Efficiency, economics, and environmental implications of phosphorus resource use and the fertilizer industry in China. *Nutrient Cycl. Agroecosyst.* 80, 131–144.
- Zhang, X.H., Jiang, W.J., Deng, S.H., Peng, K., 2009. Energy evaluation of the sustainability of Chinese steel production during 1998–2004. *J. Clean. Prod.* 17, 1030–1038.
- Zhou, J.C., Jiao, X.Q., Ma, L., de Vries, W., Zhang, F.S., Shen, J.B., 2021. Model-based analysis of phosphorus flows in the food chain at county level in China and options for reducing the losses towards green development. *Environ. Pollut.* 288, 117768.